PHYSICAL REVIEW LETTERS

VOLUME 7 OCTOBER 1, 1961 NUMBER 7

INFLUENCE OF MAGNON-PHONON COUPLING ON THE LOW-TEMPERATURE MAGNETIC PROPERTIES OF AN ANTIFERROMAGNET*

P. Pincus and J. Winter†

Department of Physics, University of California, Berkeley, California

(Received September 8, 1961)

There have been several experiments[1-4] bearing on the temperature dependence of the sublattice magnetization, parallel susceptibility, and nuclear relaxation rates of antiferromagnets. The surprising result is that, with the possible exception of MnF_2,[3] none of the experiments show any evidence for the expected energy gap[5] in the spin-wave spectrum. Furthermore, the experiments do not agree with the predictions of the usual spin-wave theory[6,7] even when the anisotropy is negligible and no energy gap is expected. The measurements[2,3] of the longitudinal nuclear relaxation time T_1 are also in disagreement with the theoretical predictions.[8] We give here a theory which is able to explain most of these results, but in terms of one coupling constant which is not too well known independently. The central idea is that the magnetostrictive terms in the Hamiltonian produce a magnon component in the thermal phonon spectrum, so that the phonons participate directly in magnetic processes.

We define the temperature T_{AE} corresponding to the energy gap by $k_B T_{AE} = \hbar\gamma(2H_e H_A)^{1/2}$, where γ is the gyromagnetic ratio, H_e the exchange field, and H_A the anisotropy field. For $T \ll T_{AE}$ the magnetic thermodynamic properties will be mainly determined by the admixture of spin-wave character into the acoustic phonons. The effective density of thermally excited magnons will then not exhibit the exponential temperature variation predicted by ordinary spin-wave theory.[5]

For the bilinear coupling between the magnons and phonons we take

$$\mathcal{H}' = G\sum_i (S_i^x S_i^z \epsilon_i^{xz} + S_i^y S_i^z \epsilon_i^{yz}), \qquad (1)$$

where G is the coupling constant and $\epsilon_i^{\mu\nu}$ the strain tensor. In a forthcoming paper[9] the transformations to the mixed magnon-phonon modes are given in detail. We have calculated the magnetic properties arising from the low-lying quasiphonons for $T \ll T_{AE}$. The deviation of the magnetization is

$$[M(0) - M(T)]/M(0) = \frac{3(6\pi^2)^{2/3} G^2 S^2}{2(\gamma H_A)^2 k_B \Theta M a^2} (T/\Theta)^4 \Gamma(4)\zeta(4), \qquad (2)$$

where M is the ionic mass; a is the lattice constant; $\Gamma(x)$ and $\zeta(x)$ are, respectively, the gamma function and Riemann zeta function; and Θ is the Debye temperature. For $\Theta = 110°K$, $a = 10^{-7}$ cm, $H_A = 10^3$ oe, and $M = 10^{-22}$ g, (2) agrees with the T^4 dependence of the sublattice magnetization observed by Poulis and Hardeman[1] in $CuCl_2 \cdot 2H_2O$ if we set $G \cong 10^{-13}$ erg. In MnF_2, Jaccarino and Walker[3] find that the observed sublattice magnetization does not seem to obey a unique power law, but (2) gives the observed order of magnitude when $G \cong 10^{-13}$ erg. In MnF_2, $H_A = 10^4$ oe, $\Theta = 450°K$, and $a \cong 3\times 10^{-8}$ cm; the other parameters are as for $CuCl_2 \cdot 2H_2O$. This contribution to the magnetization deviation is comparable with the contribution arising from the ordinary magnon branches of the spectrum in MnF_2.

For $T \ll T_{AE}$ the parallel susceptibility is proportional to the deviation of the sublattice magnetization and is given by

$$\chi_{\parallel} = (4\gamma\hbar/H_e a^3)[M(0) - M(T)]/M(0). \qquad (3)$$

The parallel susceptibility also has a T^4 temperature dependence. Such a variation has been observed by Stout and Matarrese[4] for $T \ll T_{AE}$ in CoF_2 and FeF_2; here $G \cong 10^{-12}$ erg fits the data quantitatively.

The low-lying quasi-phonon branch of the spectrum also plays an important role for the longitudinal nuclear relaxation time T_1. We calculate the direct relaxation rate,

$$1/T_1 \cong \frac{3\pi(6\pi^2)^{2/3}\hbar A^4 S^6 G^2}{2Ma^2(k_B\Theta)^4(\hbar\gamma H_A)^2}(T/\Theta), \qquad (4)$$

where A is the hyperfine coupling constant. In MnF_2, where $A \cong 10^{-18}$ erg, a relaxation rate proportional to T has been observed[3] and agrees in order of magnitude with (4) when the parameters above are used. Thus the nuclear relaxation and magnetization data find a consistent explanation. The Raman relaxation rate has a T^7 temperature dependence and agrees again with the observations[2] in $CuCl_2 \cdot 2H_2O$ where $G \cong 10^{-13}$ erg. The expression for the Raman relaxation rate is

$$1/T_1 \cong \frac{27\pi^3(6\pi^2)^{1/3}A^2S^6G^4}{16\hbar(\gamma H_A)^4M^2a^4(k_B\Theta)^3}(T/\Theta)^7 P_6, \qquad (5)$$

where A is the strength of the dipolar coupling and P_6 is given by

$$P_6 = \int_0^{x_{\max}} \frac{x^6 e^x}{(e^x-1)^2}dx; \quad x_{\max} = \hbar v k_{\max}/k_B T. \qquad (6)$$

Thus by the use of the magnon-phonon interaction we are able to explain several experiments. We require, however, somewhat larger coupling constants than have been reported in more symmetrical crystals.

The authors would like to express their appreciation to Professor C. Kittel for several valuable discussions.

---

*Work supported by the National Science Foundation.

†On leave of absence from Centre d'Etudes Nucléaires de Saclay, France.

[1]N. J. Poulis and G. E. G. Hardeman, Physica 19, 391 (1953).

[2]N. J. Poulis, G. E. G. Hardeman, and W. V. Lugt, Physica 22, 49 (1956).

[3]V. Jaccarino and L. R. Walker, J. phys. radium 20, 341 (1959).

[4]J. W. Stout and L. M. Matarrese, Revs. Modern Phys. 25, 338 (1953).

[5]J. A. Eisele and F. Keffer, Phys. Rev. 96, 929 (1954).

[6]G. Heller and H. Kramers, Proc. Roy. Acad. Sci. Amsterdam 37, 378 (1934).

[7]R. Kubo, Phys. Rev. 87, 568 (1952).

[8]T. Moriya, Progr. Theoret. Phys. (Kyoto) 16, 23 (1956).

[9]P. Pincus and J. Winter, Phys. Rev. (to be published).

RELATION BETWEEN THERMAL CONDUCTIVITY DEFECT IN SODIUM CHLORIDE AND ACOUSTIC RELAXATION EFFECTS AT LOW TEMPERATURES

K. Brugger and W. P. Mason

Bell Telephone Laboratories, Murray Hill, New Jersey

(Received August 3, 1961)

Recently an anomalously large reduction in thermal conductivity at low temperatures has been measured[1] for NaCl single crystals grown by the Harshaw process. No such reduction occurs for crystals grown free from atmospheric contamination, and evidence is presented that the reduction in thermal conductivity is associated with an impurity ion in the crystal in which oxygen is one of the components. The thermal conductivity varies nearly as the square of the temperature from 1°K to 20°K. Evidence is presented that the mean free path satisfies an equation of the type

$$\lambda = (3.3\times10^{-5}\,\omega/V)^{-1}\ \text{cm}, \qquad (1)$$

where V is the average sound velocity in the Debye sense and $\omega = 2\pi$ times the frequency of the phonon. Several mechanisms for this effect were considered but no conclusive evidence was found for any of them.

One possibility was that a relaxation process might be involved. Recently a mechanical relaxation effect has been measured at low temperatures which is associated with the same set of impurity ions, and it is the purpose of this note to show that these relaxations are in agreement with the loss in thermal conductivity.

The crystals were obtained from Harshaw and from Isomet and were provided with oriented, parallel, flat faces. X-cut and AC-cut quartz plates were bonded to the specimens with 4-methyl-1-pentene. The temperature was controlled by

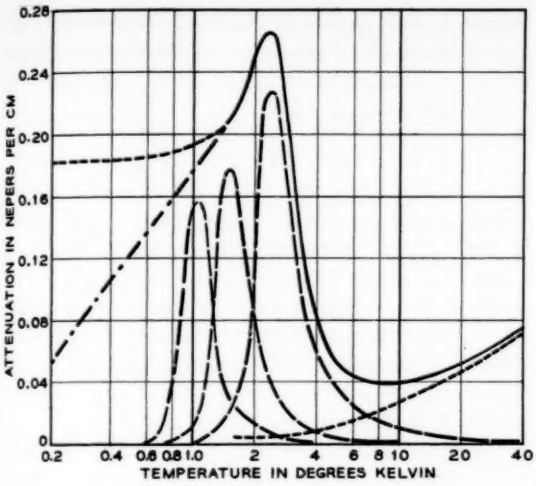

FIG. 1. Attenuation in Harshaw sodium chloride crystal for 57-Mc/sec shear wave along [110] with polarization direction [1$\bar{1}$0]. Short-dash line shows assumed background loss (due mostly to dislocations). Long-dash lines show three relaxation mechanisms.

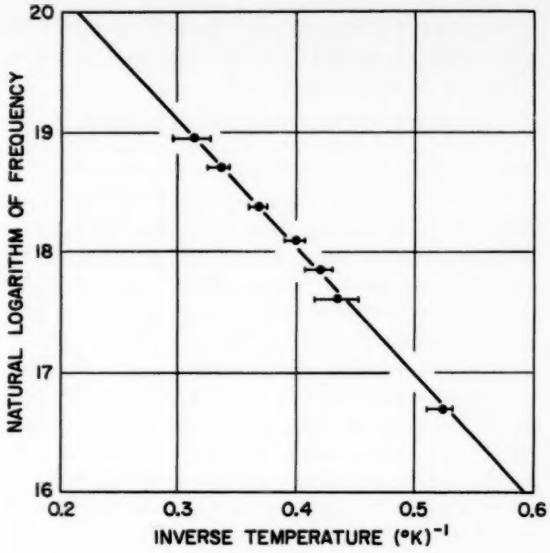

FIG. 2. Temperature shift of attenuation peak with frequency. $\ln f = \ln f_0 - E/kT$.

means of a liquid helium bath and an electric heater, and was determined from vapor pressure and carbon resistor readings. The attenuation was measured with a pulse-echo method. The relative velocity was determined using pulse overlap and a phase-comparison technique.

Figure 1, solid line, shows the attenuation in nepers per cm along the [110] direction for a 57-Mc/sec shear wave with its polarization in the [1$\bar{1}$0] direction. A large increase is seen below 5°K. No such increase was found for Isomet crystals, which are grown in a vacuum, as contrasted with Harshaw crystals, which are grown in air. It is, therefore, concluded that the observed relaxation effect is caused by a gaseous impurity introduced from air into the melt.[2] Similar conclusions on thermal conductivity were found by Klein.[1] Table I gives the number of {110} planes in which shear stresses are set up by the types of waves employed in this investigation and indicates the corresponding presence or absence of a peak. The correlation is excellent. Incidentally, the {110} planes are also the slip planes for dislocations. But in view of the small activation energy, a Bordoni relaxation effect can be discounted.

The temperature shift of the peak as a function of the frequency was measured over the range from 18 to 173 Mc/sec using shear waves polarized along [1$\bar{1}$0] and propagating along the [110] direction. The result, plotted in Fig. 2, satisfies the Arrhenius relation,

$$f = f_0 \exp(-E/RT), \qquad (2)$$

which is typical of a relaxation process. f is the

Table I. Wave types, shear stress, and attenuation in Harshaw NaCl.

Wave mode	Direction of propagation	Direction of polarization	Number of {110} planes with shear stress	Attenuation peak
Longitudinal	[100]	···	4	Yes
Transverse	[100]	in (100)	0	No
Longitudinal	[110]	···	4	Yes
Transverse	[110]	[1$\bar{1}$0]	6	Yes
Transverse	[110]	[001]	0	No

measuring frequency and T the peak temperature. The constants f_0 and the activation energy E are graphically determined to be

$$f_0 = 5\times10^{9\pm0.2} \text{ cps}, \quad E = 21 \pm 2.3 \text{ cal/mole}. \quad (3)$$

For the same shear wave, the dispersion of the sound velocity was measured at 57 Mc/sec in a Harshaw crystal as a function of the temperature. The curve obtained is typical of a broad relaxation process (at 1.5°K the value of V/V_0 is 0.9986, where V is the measured velocity and V_0 is the velocity at the broad flat maximum which stretches from 15 to 25°K).[3]

A similar attenuation curve was found for KCl at 56 Mc/sec with one maximum occurring at 5°K and a rise occurring down to 1.5°K. Unfortunately no thermal conductivity data are available for this crystal. The attenuation peaks of both crystals show some evidence of a fine structure and the width of the peaks and of the dispersion region indicate the existence of a distribution of activation energies, rather than a single one. As shown by the highest temperature long-dash relaxation curve of Fig. 1, a single relaxation agrees with the measurement above the peak temperature if we assume a background loss—mostly due to dislocations—as shown by the short-dashed line. However, at low temperatures, the indicated attenuation requires a distribution of relaxation frequencies. While the distribution may be a continuous one, a good approximation for a slowly varying attenuation is obtained by a series of relaxation energies which vary by a small ratio or increment.[4] The attempt frequency of 5×10^9 cps indicates a low probability of occurrence for the effect. A relation of the form

$$f_i = 10^{12} e^{(\Delta S_i/R)} e^{-(H_i/RT)} \quad (4)$$

is assumed for the relaxation frequency of each process. The value of 10^{12} cps is a commonly observed value for relaxation processes. For the highest energy value, ΔS has to be negative and equal to 10.6 cal/mole. The lower the activation energy H_i, the lower the disorder so that ΔS_i is assumed proportional to H_i. Then Eq. (4) becomes

$$f_i = 10^{12} e^{-0.252H_i} e^{-H_i/RT}. \quad (5)$$

The internal friction of a series of relaxation processes, and the shear modulus change associated with them, can be written in the form

$$Q^{-1} = \sum \frac{A_i(f/f_i)}{1+(f/f_i)^2}; \quad \frac{\Delta\mu}{\mu} = \sum \frac{A_i}{1+(f/f_i)^2}, \quad (6)$$

where A_i is a series of constants required to fit the shape of the attenuation curve which is related to the internal friction curve by the equation

$$\alpha = \frac{Q^{-1}\omega}{2V} = \frac{\pi f}{V}\sum \frac{A_i(f/f_i)}{1+(f/f_i)^2}. \quad (7)$$

By assuming activation energy values varying by ratios of 1.23,[4] a series of constants A_i were obtained for fitting the attenuation curve of Fig. 1 above 0.1°K. These constants were tested on the available data up to higher frequencies and reproduced the measured data with good precision. The three top relaxation mechanisms are shown by the long-dash curves of Fig. 1.

Thermal conduction occurs by means of quantized longitudinal and shear waves in the crystal of much higher frequency and these can interact with the relaxation mechanisms found by the ultrasonic measurements. Since these phonons come from all directions, on the average they will have a much smaller component of shearing strain in the {110} planes than do the waves whose attenuation is shown by Fig. 1. A calculation indicates that the factor is $\frac{1}{3}$ for shear phonons which carry most of the energy. While a complete calculation would require an integration of the distribution of frequencies occurring at each temperature, a fairly good indication is obtained by taking the dominant frequency of the distribution given by

$$hf \doteq kT \text{ or } f \doteq 2\times10^{10}T, \quad (8)$$

where h is Planck's constant and k is Boltzmann's constant. Hence, one can calculate the average distance required to cause the phonon intensity to be reduced to $1/e$ of its original value—which is one definition of the mean free path—by calculating from Eq. (7) the distance required to produce an attenuation of one neper at the frequency corresponding to the temperature T in Eq. (9). Using the measured values of α_i shown by the short-dashed curve of Fig. 1, and multiplying by the directivity factor $\frac{1}{3}$, the mean free path is shown by the solid line labelled 1 of Fig. 3. The shape of the attenuation curve at low temperatures is not very critical and the solid line of Fig. 3 labelled 2 indicates the result of a calculation for an attenuation which goes from zero at 0.1°K to the measured value at 1.4°K along the dot-dash line of Fig. 1. Either curve gives good agreement with the thermally measured value shown by the dashed line of Fig. 3, since there is no assurance that the same number of impurities occurs in each sample. The slope of the solid lines varies nearly

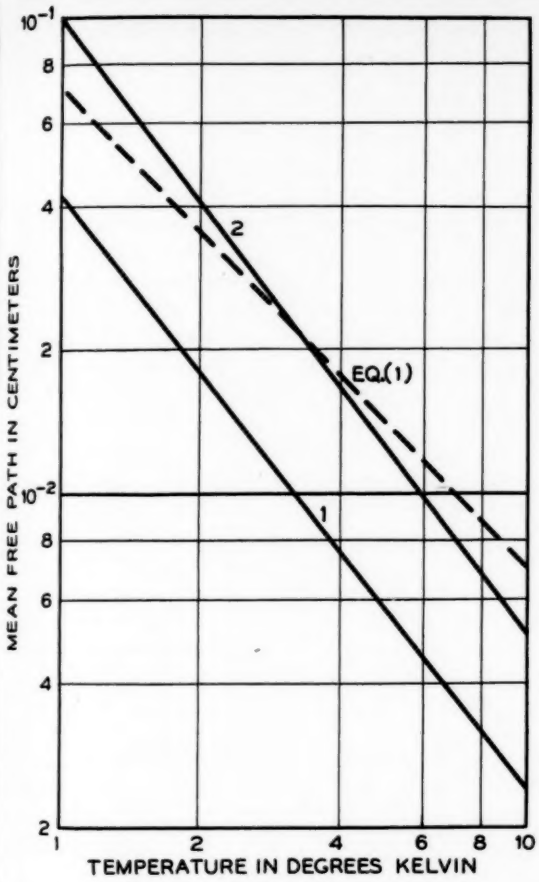

FIG. 3. Mean free path of thermal phonons. Solid line 1 calculated from dashed attenuation curve in Fig. 1. Solid line 2 calculated from dot-dash curve in Fig. 1. Dashed line represents Eq. (1).

as $T^{-1.25}$ which is actually in better agreement with the measurements[1] than the assumed slope of T^{-1}.

Thermal resistance caused by a relaxation effect appears to be a new process not covered by any of the ordinary mechanisms.[5] It appears that the change in the equilibrium states associated with the acoustic relaxation effect, produces considerable attenuation for thermal waves and a corresponding short mean free path. Since the cross section of the scattering mechanism can be obtained from the mean free path and the density of scatterers,[1] it appears that the scattering cross section for relaxation processes of this type is much larger than the size of the impurity. The very low activation energy range suggests a spectrum of normal modes of low-energy separation such as might occur for a tunneling process.

The authors wish to thank L. M. Tornillo for his help in preparing the specimens, Dr. W. Känzig for discussions of the nature of impurities in sodium chloride, and Dr. T. Kjeldaas and Dr. T. Geballe for discussions on the characteristics of thermal propagation.

---

[1]Miles V. Klein, Phys. Rev. 122, 1393 (1961).

[2]W. Känzig and M. H. Cohen, Phys. Rev. Letters 3, 509 (1959), find O_2^- ions in NaCl treated with oxygen. W. Känzig (private communication) has evidence for the presence of water in the NaCl lattice. N. R. Whellen and T. A. Vanderslice, Bull. Am. Phys. Soc. 6, 360 (1961), found CO, CO_2, and H_2O to be given off when cleaving alkali halide crystals.

[3]In Isomet crystals the sound velocity below 25°K is constant to within 1 part in 10^5.

[4]See Warren P. Mason, Physical Acoustics and the Properties of Solids (D. Van Nostrand Company, Princeton, New Jersey, 1958), Chap. X, p. 300.

[5]P. G. Klemens, in Solid State Physics, edited by F. Seitz and D. Turnbull (Academic Press, Inc., New York, 1958), Vol. 7, pp. 1-98.

ENHANCEMENT OF SUPERCONDUCTIVITY BY EXTRACTION OF NORMAL CARRIERS

R. H. Parmenter
RCA Laboratories, Princeton, New Jersey
(Received August 1, 1961)

One can ask the question: Why does a sufficiently high temperature always lead to quenching of superconductivity in a metal? An examination of the Bardeen-Cooper-Schrieffer (BCS) theory of superconductivity[1] shows that the answer to this question is as follows: The phonon-induced electron-electron attraction between electrons leads to a resonant, or coherent, interaction between the one-electron states of the metal. The greater the number of states interacting, the greater will be the resonant interaction, and thus the greater the lowering of the energy of the assembly of superconducting electrons of the metal. As the temperature is raised, electrons are thermally excited out of this sea of superconducting electrons, thus giving rise to normal electrons and holes. The one-electron states occupied by these normal carriers are no longer available for the resonant interaction (because of the exclusion principle), thereby decreasing the strength of the resonant depression of the energy of the system. At a sufficiently high temperature (the superconducting transition temperature), there are sufficient normal carriers present to quench the resonance completely, whereupon the metal becomes normal.

This suggests that, if there were some method of electrically extracting the normal carriers as soon as they are thermally generated, then it might be possible to maintain the metal superconducting above the usual transition temperature. As a result of recent work,[2] it is known that it is indeed possible to inject or extract normal carriers from a superconductor. (It is this phenomenon which insures the success of the operation of the superconducting tunnel diode.) This is done by making contact to another superconductor through a thin (10-20 angstroms) insulating layer, the latter serving to pass normal carriers under suitable bias (by tunneling), but to block superconducting electrons completely. It appears that an insulating barrier more than a few angstroms thick is effective in preventing current flow involving the cooperative motion of many electrons (i.e., the superconducting current) while at the same time allowing some current flow involving uncorrelated motions of individual carriers (i.e., the normal current).

Let us suppose we wish to extract normal carriers from superconductor A having transition temperature T_{cA}. We assume that the operating temperature T is close to (but smaller than) T_{cA} in order that there be appreciable numbers of normal carriers in A under equilibrium conditions. Through a thin insulating layer, we make contact with superconductor B having transition temperature T_{cB} sufficiently greater than T for there to be negligible numbers of normal carriers present in it. By now biasing such a diode with a voltage equal to one-half the energy-gap difference of the two superconductors, we can extract either normal electrons or normal holes (depending on the polarity of the bias) from A. By having A in the form of a film sandwiched between contacts (electrodes) of superconductor B (along with the thin insulating layers), we can extract both signs of normal carriers by putting a bias between the two B contacts equal to or greater than the energy-gap difference $2(\epsilon_{0B}-\epsilon_{0A})$. If the bias is made greater than the energy-gap sum $2(\epsilon_{0B}+\epsilon_{0A})$, however, we get an additional effect due to generation of isoenergetic electron-hole pairs at each insulating interface—this effect leading to a double injection of normal carriers into A. This injection apparently will overbalance the previously discussed double extraction, so that for biases greater than $2(\epsilon_{0B}+\epsilon_{0A})$, there will be a net injection rather than extraction. Figure 1 illustrates the energy-level diagrams for such a device under conditions of zero, $2(\epsilon_{0B}-\epsilon_{0A})$, and $2(\epsilon_{0B}+\epsilon_{0A})$ bias.

We designate by τ the lifetime against normal electron-hole recombination and by n' the density of normal electrons (or holes) in a superconductor under thermal equilibrium conditions. Thus n'/τ is the normal electron-hole pair generation rate per unit volume in the superconductor. (It is also the recombination rate.) Under conditions of extraction in the superconductor, we shall, for the moment, assume the normal pair generation rate is unchanged (i.e., that it remains n'/τ). The recombination rate, however, will be reduced to $(n''/n')^2(n'/\tau)$, where n'' is the reduced density of normal electrons resulting from the extraction process. The factor $(n''/n')^2$ is a consequence of the fact that we are dealing with a bimolecular recombination process. We designate by L the thickness of the superconducting film

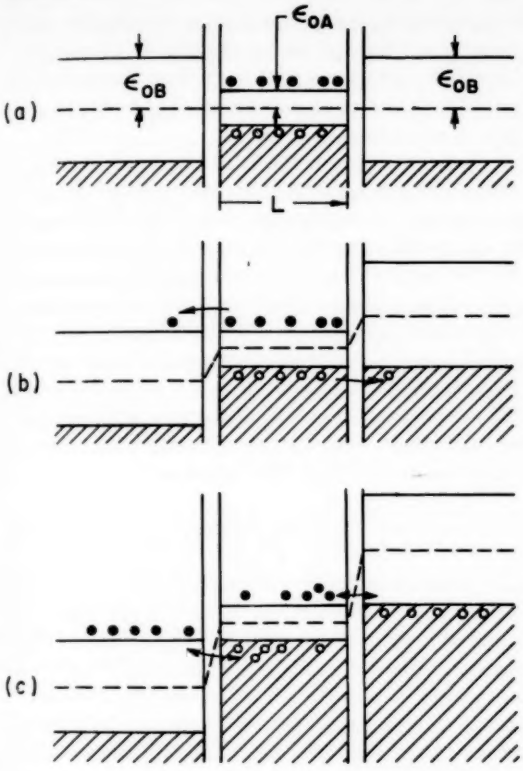

FIG. 1. Energy level diagrams for a system of a superconducting film of thickness L and energy gap $2\epsilon_{0A}$ separated by insulating layers from superconducting contacts having energy gap $2\epsilon_{0B}$. (a) Zero bias. (b) Bias $= 2(\epsilon_{0B} - \epsilon_{0A})$. (c) Bias $= 2(\epsilon_{0B} + \epsilon_{0A})$.

being subjected to extraction, by γ the mean tunneling transition probability per collision of the normal carriers striking the insulating barriers, and by v_F the velocity of the normal carriers (this being the Fermi velocity). The pair extraction rate per unit volume of superconducting film is $\frac{1}{2}v_F(n''/2)(\gamma/L)$. Upon setting the difference between the generation rate and the recombination rate equal to the extraction rate (i.e., dynamic equilibrium), we get

$$\left[1 - \left(\frac{n''}{n'}\right)^2 - \left(\frac{\gamma\lambda}{6L}\right)\left(\frac{n''}{n'}\right)\right]\left(\frac{n'}{\tau}\right) = 0, \qquad (1)$$

where $\lambda = v_F\tau$ is the mean free path against pair recombination under thermal equilibrium conditions. If $\gamma\lambda/6L \gg 1$, then

$$n''/n' = 6L/\gamma\lambda \ll 1, \qquad (2)$$

and the extraction process is very efficient. An order-of-magnitude lower limit to λ is given by the normal-state bulk electrical conductivity mean free path λ_n as limited by lattice vibrations, λ_n being a lower limit since it is harder to generate normal pairs thermally in a superconductor than in the corresponding normal metal. The real phonon absorbed in the generation process must have at least the gap energy in the case of the superconductor. Thus if the operating temperature is appreciably below the usual transition temperature of the superconductor, we can expect $\lambda \gg \lambda_n$. Since λ_n may be 10^{-2} cm and $\gamma \sim 10^{-2} - 10^{-3}$ under typical conditions, Eq. (2) shows that L, the superconducting film thickness, may be 100 angstroms or more and still have $(n''/n') \ll 1$.

In carrying out the analysis of the extraction process, we have assumed spatial uniformity of n'' in the superconducting film. This will be an excellent approximation as long as $L \ll \lambda$. We also assumed the pair generation rate to be unaffected by the extraction process. As we shall see in a moment, however, the superconducting energy gap may increase under conditions of extraction. If so, this implies a decrease of the generation rate with increasing extraction (fewer phonons are energetic enough to create pairs). Such a decrease of the generation rate obviously does not invalidate the conclusions of the preceding paragraph.

A third assumption is that the density of normal carriers in the contacts is negligible compared with n'', the density in the superconducting film, so that there is negligible tunneling of normal carriers from the contacts back into the film. This implies that there is an efficient method of getting rid of the normal carriers injected into the contacts. One way of accomplishing this is to plate each contact with a certain amount of normal metal. The latter will serve as an efficient sink for normal carriers injected into the contact, whenever the distance from the tunnelable barrier facing the contact is less than a mean free path (for normal carriers in S_B) from the normal metal of the contact. The normal metal should be separated from the tunnelable barrier by a thickness of superconductor B of at least something of the order of the Pippard coherence distance (10^{-4} cm), and the normal metal itself should have minimum thickness of similar size. This obviates the possibility that the normal metal is made superconducting by being in contact with S_B, or conversely that S_B has its superconductivity quenched by being in contact with a

normal metal.[3]

It should be pointed out that the superconductor S_B in each contact contains injected normal electrons or normal holes, but not both. (One contact will have electrons, and the other holes.) The resulting space charge in each contact will be compensated by an adjustment in the density of superconducting electrons (a shift of the energy of the bottom of the conduction band in S_B relative to the Fermi level). This will lead to a minute shift in the transition temperature of each contact.[4] Such a shift will be negligible compared with the shift of transition temperature of the superconducting film S_A due to extraction of normal carriers of both signs without change of the density of superconducting electrons.

The situation we are considering in this note represents a nonequilibrium condition. There are two general types of nonequilibrium conditions in a superconductor: (1) those where the lack of equilibrium is due to the superconducting electrons, so that dissipation processes do not occur; (2) those where the lack of equilibrium is due to the normal carriers, so that dissipation processes do occur (i.e., finite entropy production). Time-independent current flow in a superconducting wire is an example of the first type.[5] Because of the lack of dissipation, it is possible to define a free energy, despite the lack of equilibrium. Specifically, one modifies the equilibrium free energy by adding a term equal to the product of the quantity being constrained times a Lagrangian multiplier. (The constraint, set by boundary conditions, is what causes disequilibrium.) For the example of dc current flow in a superconducting wire, the constraint is that imposed on the net current due to the superconducting electrons.[6]

The extraction of normal carriers represents a nonequilibrium situation of the second type where dissipation processes occur. There is a certain amount of thermoelectric cooling in the superconducting film being exhausted of normal carriers, and a still greater amount of heating in the contacts. For example, under the bias conditions of Fig. 1(b), heat is being removed from the film at the rate $I(2\epsilon_{0A}/e)$ and being liberated in each contact at the rate $I(\epsilon_{0B}/e)$ when extraction is efficient. (Here I is the total current, and e is the electronic charge.) The removal of heat in the film occurs when phonons are absorbed in making normal hole-electron pairs. Because of backflow of heat from the contacts into the film, the actual temperature drop of the film is probably small enough to ignore. Nevertheless, the presence of dissipation associated with this thermoelectric process makes it difficult to define any sort of free energy F such that the minimization of F will lead to a description of steady-state equilibrium.

A generalization of the BCS theory to such a nonequilibrium situation can be made in the following manner. A Boltzmann transport equation is set up for the distribution function f_k associated with the normal carriers (normal electrons for $k > k_F$, and normal holes for $k < k_F$, $\vec{k}$ being the wave vector labeling the single-particle states, and k_F being the Fermi wave vector). At the same time, the internal energy U is minimized with respect to the parameters h_k appearing in the BCS many-electron wave functions.[7] Such a minimization leads to the equation

$$[N(0)V]^{-1} = \int_0^{\hbar\omega} (\epsilon_k^2 + \epsilon_0^2)^{-1/2} (1 - 2f_k) d\epsilon_k. \qquad (3)$$

Here $N(0)V$ and $\hbar\omega$ are constraints characteristic of the superconductor, ϵ_k is the single-electron Bloch energy (measured with respect to the Fermi level), $2\epsilon_0$ is the energy gap, and $(\epsilon_k^2 + \epsilon_0^2)^{1/2}$ is the energy of a normal carrier in the superconductor (also measured with respect to the Fermi level). Equation (3) is formally the same as that of the BCS theory; the only difference lies in the fact that the f_k contained therein is obtained from a Boltzmann transport equation rather than from a minimization of a free energy with respect to f_k.

Of course, it is possible to have a nonequilibrium situation where both the superconducting electrons and the normal carriers contribute to the disequilibrium. For such a situation, one should solve a Boltzmann equation for f_k and at the same time minimize the internal energy U with respect to h_k subject to the constraint on the superconducting electrons causing their disequilibrium. Such a situation arises in the particular physical problem of the superconducting film with extracting electrodes if we choose to make a supercurrent flow in the film parallel to the plane of the film at the same time that we are extracting normal carriers from the film.

For the moment, we return to the case where there is no supercurrent in the superconducting film. Boltzmann's equation for our problem reduces to the statement that the total time rate of change of f_k vanishes, the three processes of normal-pair thermal generation, normal-pair recombination, and double extraction of normal carriers all contributing to (df_k/dt). The extrac-

tion process is effective in lowering f_k for all orientations of $\vec{k}$, despite the fact that only carriers moving nearly normal to the insulating interface have appreciable probability of tunneling. This lowering of f_k for all orientations is a consequence of the fact that those carriers reflected at the insulating interface are undoubtedly reflected diffusely, thus leading to rapid equilibration between isoenergetic carriers moving in different directions.

It is not really necessary to solve Boltzmann's equation for f_k. Under reasonable physical conditions, it appears that whenever extraction is efficient as a whole, i.e., whenever $(n''/n') \ll 1$, it will also happen that

$$f_k \ll 1. \qquad (4)$$

This will hold for all $\vec{k}$ if the bias is adjusted such that normal carriers of all energies can tunnel [e.g., as in Fig. 1(b)]. [In contrast, under no-extraction conditions where n' is appreciable, there will be a number of f_k comparable with $\frac{1}{2}$ and thus not satisfying (4).] It should be noted that the only way the temperature T can affect the energy gap $2\epsilon_0$, obtained by solving Eq. (3), is through the temperature dependence of f_k. However, as long as (4) holds true, then (3) will be independent of T, and we will obtain an ϵ_0 equal to the BCS value at the absolute zero of temperature, even when T is above the usual superconducting transition temperature.

It would appear that, by means of electrical extraction, we can raise the transition temperature of the superconducting film. An upper limit to this new transition temperature will, of course, be set by T_{cB}, the transition temperature of the contacts. As the operating temperature approaches T_{cB}, the extraction efficiency will drop off because of the presence of thermally generated normal carriers in the contacts which may tunnel through the insulating layers into the superconducting film. It appears plausible that one should be able to start with the film in the normal state and by means of extraction cause the film to go superconducting, the operating temperature being less than T_{cB} but greater than T_{cA} (the usual transition temperature of the film). Conversely, we should be able to lower the transition temperature of the film by injection of normal carriers as shown in Fig. 1(c). By lowering the transition temperature below the operating temperature, we can drive the superconducting film normal by electrical injection. Using either injection or extraction, we have an electrical (nonmagnetic) method of controlling a superconducting current in the film (the current flowing parallel to the plane of the film).

---

[1]J. Bardeen, L. N. Cooper, and J. R. Schrieffer, Phys. Rev. 108, 1175 (1957).

[2]J. Nicol, S. Shapiro, and P. H. Smith, Phys. Rev. Letters 5, 461 (1960); I. Giaever, Phys. Rev. Letters 5, 464 (1960); I. Giaever and K. Megerle, Phys. Rev. 122, 1101 (1961).

[3]R. H. Parmenter, Phys. Rev. 118, 1173 (1960); P. H. Smith, S. Shapiro, J. L. Miles, and J. Nicol, Phys. Rev. Letters 6, 686 (1961).

[4]R. E. Glover, III, and M. D. Sherrill, Phys. Rev. Letters 5, 248 (1960).

[5]J. Bardeen, Phys. Rev. Letters 1, 399 (1958).

[6]In reference 5, it appears that the constraint is being imposed on the normal current rather than the superconducting current. This is because the calculation, for convenience, is being carried out in a coordinate system moving with the mean drift velocity of the superconducting electrons. In the laboratory coordinate system, the constraint is being imposed on the supercurrent, not the normal current.

[7]The internal energy U is formally the same as in the BCS theory, i.e., Eq. (3.16) of BCS after removal of the term $-TS$. In the BCS theory, the free energy $F = U - TS$, rather than U, is minimized with respect to h_k. This difference is of no consequence, since the entropy S is independent of h_k. The minimization of U with respect to h_k appears to be the only reasonable way of generalizing the BCS variational approach to a nonequilibrium situation. Such a minimization nevertheless represents an assumption.

SUPERCONDUCTIVITY OF SUPERIMPOSED METALS*

A. C. Rose-Innes† and B. Serin
Rutgers University, New Brunswick, New Jersey

(Received September 1, 1961)

Measurements[1-3] on thin films of superconductors in contact with normal metals have shown that the transition temperature of the films is lowered. For sufficiently thin films the transition temperature may be reduced to such an extent that superconductivity is not observed. There have been several theories of this effect.[1,4,5] Our experiments described here indicate that for films deposited by evaporation the effects observed can be considerably influenced by diffusion between the two metals.

We have made a series of measurements of the magnetic moment of superconducting tin films evaporated onto gold plates. The method used to detect the magnetic moment was similar to Alekseyevsky's,[6] in which the specimen is suspended from a torsion balance at a small angle to a uniform magnetic field. As the field strength is increased the film rotates until it is parallel to the field. The deflection is then constant until the critical field value is reached, when the specimen returns to its original position. This method is preferable to the measurement of resistance which has been used in all previous experiments. The resistance method has the disadvantage that it may not necessarily measure a bulk property of the film. Zero resistance may arise from superconducting filaments, or a finite resistance may result from small breaks in the film, neither of which is characteristic of the material as a whole. However, the magnetization is a bulk property, not affected by small discontinuities. Moreover, measurements of the magnetic moment as a function of temperature and magnetic field show whether or not the specimens behave like films of an ideal superconductor.

The substrates for our films were 99.99% pure gold plates 21 mm × 21 mm and of thickness 0.25 mm. The plates were annealed at 750°C for about a day and then wiped with trichlormethylene. During the evaporation they were firmly clamped to a hollow copper block cooled by flowing water at room temperature. The tin was evaporated from a molybdenum boat about 15 cm below the plate. During evaporation the pressure was less than 5×10^{-5} mm Hg. At the same time, the film was also deposited onto a thin glass cover slip which was next to the gold plate and symmetrically placed with respect to the boat. Between the boat and the plates was a shutter which was opened only after the tin had been melted, outgassed, and evaporation had begun. The shutter was kept open for 2.5 min for all evaporations so that every specimen saw the hot boat for the same length of time. The electrical power supplied to the boat also was the same for all depositions.

The anount of tin placed in the boat was weighed to give the thickness desired, and the evaporation time was sufficient to insure that all the tin vaporized. Thicknesses quoted in Table I were determined by weighing the glass slips before and after deposition. The films were squares of area about 3 cm^2.

Table I shows the results of the measurements on these films. There is a rapid decrease in transition temperature when the thickness of tin is less than about 7000 A; also, the films fall into two groups. Those specimens with transition temperatures close to the value of bulk tin (say $T_c > 3.4$°K) had sharply defined critical magnetic fields, and the magnetization and critical fields exhibited the behavior to be expected for thin films of an ideal superconductor. However, those films whose transition temperatures were appreciably depressed showed the characteristics of nonideal superconductors, having very high critical fields which were not sharply defined. Furthermore, their magnetic moments were smaller than those of the other films. The films deposited onto glass all had transition temperatures near the

Table I. Superconducting properties of tin films on gold.

Film	Thickness (A)	T_c (°K)	Behavior
5	18 700 ±500	3.71	ideal
8	13 200	3.40	ideal
9	9500	3.51	ideal
10	7800	2.68	nonideal
13	7100	3.57	ideal
14	7100	3.59	ideal
15	6100	3.08	nonideal
11	6100	1.66	nonideal
7	5700	not superconducting down to 1.35°K	
6	1500		
4	1500		

value of bulk tin.

These results appeared to confirm qualitatively the earlier observations of this effect. Misener and Wilhelm[1] found that tin films electroplated on constantan ceased to be superconducting above 2°K at thicknesses less than 3000 A. More recently, Meissner[2] measured several pairs of metals, including tin on gold, and reported a critical thickness of a few hundred angstroms. Smith, Shapiro, Miles, and Nicol[3] observed qualitatively similar effects with lead and silver films.

However, by further experiments we showed that under the conditions of our evaporations diffusion probably occurred despite the cooling precautions. This was established by replacing some of the specimens in the evaporator and exposing the films to the radiation from the hot empty boat, under conditions similar to those used in laying them down. After this treatment we measured their superconducting properties again and found them changed. The transition temperature of film 14 was reduced to 2.26°K after a 2.5-min exposure, and its magnetic behavior changed from ideal to nonideal in the sense already explained. After a further exposure of 2.5 min, film 14 was not superconducting down to 1.27°K. Film 9 after a 5-min exposure was not superconducting down to 1.23°K. The appearance of the films was unchanged after these exposures. Since the superconductivity of our films can be destroyed by heating the tin-gold surface, it follows that the value of the thickness at which the transition temperature is observed to fall rapidly has no particular significance, but is a consequence of the way the specimens were prepared.

We believe that the effects of reheating show that diffusion can easily occur during evaporation, and result in a decreased transition temperature. Furthermore, diffusion might account for the different values given by various workers for the thickness at which superconductivity disappears. The degree of diffusion and alloying which can take place will, of course, depend on the particular pair of metals used and the method of film deposition.

Gold is only soluble in tin up to 0.3% and about 4% of tin is soluble in gold, but intermetallic compounds $AuSn_4$ and $AuSn_2$ exist.[7] Allen[8] studied the superconductivity of tin-gold alloys and found that the transition temperature of the tin-rich alloys is independent of gold concentration up to about 30% gold. The intermetallic compounds are also superconducting, but alloys with more than 50% gold are not superconducting down to 1.5°K.

Although diffusion seems to reduce the transition temperature, the exact reason for this is not obvious. Appreciable interpenetration of the two metals could have two effects: Nonsuperconducting alloys may be formed; or the thickness of the superconducting metal could be reduced to a value much less than that deduced from the weight. Alternatively, there may be only a small interpenetration resulting in more perfect contact between the two metals,[9] which according to Cooper[5] can lower the transition temperature of relatively thick films.

In conclusion, we feel that we have shown that diffusion can play a critical role in experiments on the superconductivity of superimposed metals; and consequently, great caution must be used in the interpretation of such experiments until the role which diffusion plays is adequately understood.

We are grateful to Miss S. Goldis for her assistance in these experiments.

---

*This work was supported by the National Science Foundation.

†Harkness Fellow of the Commonwealth Fund, on leave from The Services Electronics Research Laboratory, Baldock, Herts, England.

[1]A. D. Misener and J. O. Wilhelm, Trans. Roy. Soc. Can. III. 29, 5 (1935).

[2]H. Meissner, Phys. Rev. 117, 672 (1960).

[3]P. H. Smith, S. Shapiro, J. L. Miles, and J. Nicol, Phys. Rev. Letters 6, 686 (1961).

[4]R. H. Parmenter, Phys. Rev. 118, 1173 (1960).

[5]L. N. Cooper, Phys. Rev. Letters 6, 689 (1961).

[6]N. E. Alekseyevsky, J. Tech. Phys. U.S.S.R. 4, 401 (1941).

[7]M. Hansen, Constitution of Binary Alloys (McGraw-Hill Book Company, Inc., New York, 1958), 2nd ed., p. 233.

[8]J. F. Allen, Phil. Mag. 16, 1005 (1933).

[9]We are indebted to Dr. Cooper for suggesting this possibility.

ABSENCE OF ANTIFERROMAGNETIC DOMAIN WALLS IN MnF_2

P. S. Pershan
Gordon McKay Laboratory, Harvard University, Cambridge, Massachusetts
(Received September 5, 1961)

It has been suggested that the electrically induced shift of the F^{19} nuclear resonance frequency in MnF_2 can be used to study the presence or absence of antiferromagnetic domain walls.[1] The purpose of this note is to report the absence of domain walls in a single crystal of MnF_2.

In MnF_2, below the Néel temperature, the antiferromagnetic ordering of the Mn^{++} ions causes a large internal magnetic field at the F sites; at 4.2°K, with no applied magnetic field, the F nuclei resonate at 159.970 Mc/sec.[2]

Figure 1 shows two alternate choices for the unit cell of MnF_2, depending on which Mn^{++} ion is chosen for the corner. For the F nuclei at *A* sites, the three nearest Mn^{++} ions in $(1\bar{1}0)$ planes and their magnetic moments are oriented so the local field at the F is up. For the *B* sites the three nearest neighbors are in (110) planes and the local field is down.[3]

An electric field in the [110] direction will split the nuclei at *A* sites by 1.4 kc/sec per volt/cm but leave the *B* sites unaffected.[1] A magnetic field in the [001] direction, as shown, and no electric field, will increase the resonance frequencies of the nuclei at *A* sites by 4 kc/sec per gauss and decrease the ones at *B* sites by the same amount. If both these fields are simultaneously applied, the resonance frequencies of the nuclei at *A* sites will increase and split into a doublet while the nuclei at *B* sites will decrease their frequency and remain unsplit.

If, however, the crystal has another domain, the Mn^{++} magnetic moments in that domain will be antiparallel to the arrows in Fig. 1. When the field *H* is applied as shown, the resonance frequency of the nuclei at *A* sites will decrease rather than increase. For the electric and magnetic fields as shown, this domain would have a doublet at a lower frequency than the singlet. Superposition of the resonances from both domains would result in two triplets; the relative strength of the outer to inner components of the triplet is a measure of the fraction of crystal taken up by each domain. For a multidomain crystal both types of domains occupy equal volume and the central component of the triplet is twice as big as the outer components.

The crystal was cut from a single crystal of MnF_2 as a plane parallel slab 1 mm×4.8 mm ×7.9 mm with the [110] direction perpendicular to the broad face. Electrodes were applied to the broad face as described in reference 1. The resonances were observed with the spectrometer built by Kushida for the pressure dependence of the F resonance in MnF_2.[4] The spectrometer was frequency swept by a motor-driven capacitor and frequency modulation was used to record the first derivative of the lines. It was not possible to operate the spectrometer without some degree of saturation; hence one must exercise caution in trying to interpret linewidth and amplitude variations of the traces in Fig. 2. The magnetic field was supplied by a small permanent magnet.

The resonance in Fig. 2(a) is with no external

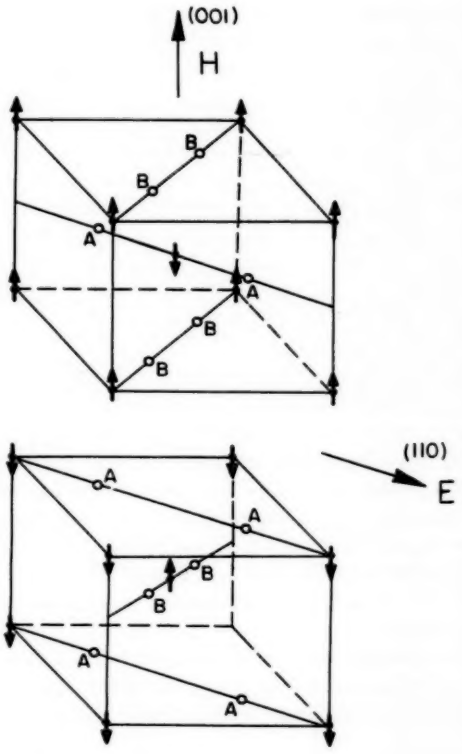

FIG. 1. Two alternate choices for the unit cell of MnF_2, depending on the particular Mn^{++} ion chosen for a corner position. The arrows indicate the orientation of the time-averaged magnetic moment for the Mn^{++} ion.

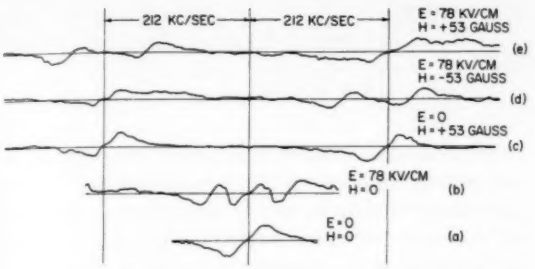

FIG. 2. The F^{19} nuclear resonance signal with various combinations of electric and magnetic fields.

fields. In Fig. 2(b) the line is split by an electric field in the [110] direction; the doublet due to spins at *A* sites combine with a singlet from spins at *B* sites to form a triplet. For Fig. 2(c) the magnetic field is on and the electric field is off. Figure 2(d) has both electric and magnetic fields applied as shown in Fig. 1. If we compare the shape of the doublet with the triplet in Fig. 2(b), there is no evidence for more than one domain. With the signal-to-noise level available, we can conclude that more than 80% of the crystal is of one domain type. In Fig. 2(e) the magnetic field is reversed interchanging the singlet and doublet. The singlets in 2(d) and 2(e) seem to be broadened by the electric field much more than either component of the doublets. This is expected since the singlets are sensitive to misorientation of the electric field to the first order while the doublets have only a second-order dependence.

These same results were obtained on two occasions. The only difference was that, on warming up and recooling below the Néel temperature, the two sublattices reversed direction.

Absence of domain walls in perfect crystals of MnF_2 at 4.2°K is expected on the basis of theoretical calculation of Li.[5] The large anisotropy forces in MnF_2 require a domain wall to be only one lattice spacing thick. There is no reduction in the magnetostatic energy to compensate for this large increase in the exchange energy and the gain in entropy on creating a domain wall is not large enough to make the change in free energy negative.

Antiferromagnetic domains can, and probably do, exist for some time after the crystal is first lowered through the Néel point. Well below the Néel point they are thermodynamically unstable, however, and unless pinned down by some sort of lattice inperfection they diffuse themselves out of existence.

The stability and motion of domain walls near the Néel point has recently received theoretical attention.[6] Observations of the F^{19} nuclear resonance just below the transition temperature show linewidths up to 600 kc/sec.[7] This is much larger than the maximum electric field splitting observable in MnF_2. The linewidth, however, is a strong function of temperature and it should be possible to search for domain walls about 10°K below the Néel point.

This research was stimulated by discussions with Professor N. Bloembergen and grateful acknowledgment is given for his contribution.

---

[1]P. S. Pershan and N. Bloembergen, Phys. Rev. Letters (to be published).

[2]V. Jaccarino and R. G. Shulman, Phys. Rev. 107, 1196 (1957).

[3]R. G. Shulman and V. Jaccarino, Phys. Rev. 108, 1219 (1957).

[4]G. B. Benedek and T. Kushida, Phys. Rev. 118, 46 (1960).

[5]Yin-Yuan Li, Phys. Rev. 101, 1450 (1956).

[6]J. W. Cahn and R. Kikuchi, J. Phys. Chem. Solids 20, 94 (1961).

[7]Peter Heller, Harvard University (private communication).

NATURE OF THE V_1 CENTER

Frederick Seitz
Department of Physics, University of Illinois, Urbana, Illinois
(Received September 11, 1961)

The V_1 center, discovered by Casler, Pringsheim, and Yuster[1] in 1950, has been the object of much speculation. Operating within the framework of pure vacancy models, which seemed most appropriate a decade ago, the writer[2] proposed that this center is the antimorph of the F center, consisting of a positive-ion vacancy and a hole. In the meantime, the experimental work of Känzig, Woodruff, and Castner[3] and Delbecq, Smaller, Yuster, and Hayes[4] has made it increasingly clear that many centers of the V type very probably involve interstitial halogen atoms, in keeping with a general conjecture first put forward by Varley.[5] In particular it seems highly probable that the H and V_1 centers, which are closely related, are of this type. Kingsley,[6] in connection with his extensive study of the centers, has given evidence to show that the present author's model of the V_1 center may well be assigned more appropriately to the experimentally observed V_4 center.

There is strong support for the view that the H center is a neutral halogen atom in a crowdion configuration in a (110) row of halogen ions. Presumably the center is normally produced in close juxtaposition to an F, F', or α center when generated by excitation of the electronic structure of the lattice. Känzig, Castner, and Woodruff[3] have proposed that the V_1 center is a neutral halogen molecule in a vacant halogen site—a model which faces numerous difficulties. Cape[7] has proposed another model. It seems hopeless at present to propose a logically water-tight model of the V_1 center which ties together in a highly precise way all of the observations made on different crystals of varying perfection in different laboratories by different observers. It seems to the author, however, that the model which combines the maximum degree of simplicity with the minimum number of major contradictions is based on the view that the V_1 center is an interstitial negative ion, presumably surrounded tetrahedrally by like and unlike neighbors [i.e., at a $(\frac{1}{4}, \frac{1}{4}, \frac{1}{4})$ position]. It is assumed that this center migrates by interstitialcy diffusion when the V_1 band bleaches so that the Dutton-Maurer current[8] is electrolytic. Since the interstitial ions should be close to halogen-vacancy partners initially, it is reasonable to expect[9] the current peak to be displaced from the annealing peak for optical absorption, provided the V_1 centers are annihilated at F or α centers at the terminus of migration. It is assumed that the conversion from H to V_1 in warming from liquid helium to liquid nitrogen range of temperature involves the transfer of an electron from an F center to an H center to form an energetically more stable vacancy-interstitial pair. It should be stated that this model was mentioned in passing by Kingsley,[6] but was discarded for reasons which possibly are too severe. Some of its principal virtues are as follows:

1. The absence of electron spin.
2. The absence of dichroism.[10]
3. It is negatively charged so that it will not capture photoelectrons from F or F' centers.
4. F' centers are immune to annihilation by migrating V_1 centers but F and α centers are not.
5. The absence of an observable Hall current when migration starts.
6. It is a natural complement to the halogen-vacancy centers so that there is no residual interstitial when it combines with an α or F center.
7. One may reasonably expect it to migrate under repeated optical excitations.

Apart from questions relating to the relative stability of the V_1 center proposed here, the model faces the following major obstacles:

1. The V_1 center does not show appreciable photoconductivity, as one might naively expect from its negative charge and by analogy with the F' center. Actually this appears to be a delicate problem since the center has an appreciable Coulomb-like polarization field. It is possible that the first excited state is stable.
2. One wonders why the V_1 center does not blunder into some of the V_k centers (self-trapped holes) when they migrate and annihilate a significant fraction of the latter. If they did, H centers would be produced.
3. Kingsley[6] points out that if an interstitial halogen ion were to meet an F center, a free electron which could annihilate a V_k center would be produced whereas no such effect appears to be observed. This matter remains open for question.

The model might be tested in KBr by seeing if additions of KCl inhibit both thermal bleaching and charge flow associated with V_1. Presumably interstitial Cl^- ions, once formed, would trap the

interstitialcy pattern.

There has been frequent discussion[11] of the manner in which excitation of the electronic system may lead to the generation of vacancy-interstitial pairs in the halogen lattice. It may not be out of place to point out that an α center (a halogen-ion vacancy) is created when a U center (a negative hydrogen ion in the site of a halogen ion) is excited with light at low temperatures.[12] It follows that the excited hydrogen ion is sucked into an interstitial position as a result of the forces of attraction between it and the normal halogen ions of the lattice. There seems to be no fundamental reason why this should not occur to an excited halogen ion under appropriate conditions.[13] Thus a self-trapped exciton may spontaneously generate a halogen-ion vacancy and an interstitial halogen ion. In the case of the halogen, the generation of the interstitial configuration could involve interstitialcy motion, the ion initially at the site of the vacancy moving to a normal nearest-neighbor position.

The author is indebted to Dr. Lüty for a discussion of this topic.

---

[1]R. Casler, P. Pringsheim, and P. H. Yuster, J. Chem. Phys. 18, 887, 1564 (1950).

[2]F. Seitz, Phys. Rev. 79, 529 (1950).

[3]W. Känzig, Phys. Rev. 99, 1890 (1955); T. G. Castner and W. Känzig, J. Phys. Chem. Solids 3, 178 (1957); T. O. Woodruff and W. Känzig, J. Phys. Chem. Solids 5, 268 (1958); W. Känzig and T. O. Woodruff, J. Phys. Chem. Solids 9, 70 (1958); Phys. Rev. 109, 220 (1958).

[4]C. J. Delbecq, B. Smaller, and P. H. Yuster, Phys. Rev. 111, 1235 (1958); W. Hayes and G. M. Nichols, Phys. Rev. 117, 993 (1960); C. J. Delbecq, W. Hayes, and P. H. Yuster, Phys. Rev. 121, 1043 (1961).

[5]J. H. O. Varley, J. Nuclear Energy 1, 130 (1954).

[6]J. Kingsley, thesis, University of Illinois, 1960 (unpublished); Phys. Rev. 122, 772 (1961).

[7]J. A. Cape, Phys. Rev. 122, 18 (1961). He proposes that the V_1 center is an H center that has been trapped at or near a positive-ion vacancy after migrating. This model has many virtues but apparently leaves the charge burst unexplained; moreover, one might expect it to be paramagnetic.

[8]D. Dutton and R. J. Maurer, Phys. Rev. 90, 126 (1953); G. Chiarotti and N. Inchauspé, Phys. Rev. 109, 345 (1958).

[9]See, for example, R. C. Fletcher and W. L. Brown, Phys. Rev. 92, 585 (1953); F. Seitz and J. S. Koehler, Solid State Physics, edited by F. Seitz and D. Turnbull (Academic Press, Inc., New York, 1956), Vol. 2, p. 366.

[10]However, P. H. Yuster informs me that V_1 centers probably show some anisotropy with (110) orientation when bleached at liquid helium temperatures. This does not appear at liquid hydrogen, or higher, temperatures.

[11]See reference 5; C. C. Klick, Phys. Rev. 120, 760 (1960); F. E. Pretzel and R. L. Petty, Phys. Rev. 123, 464 (1961).

[12]H. Thomas, Ann. Physik 38, 601 (1940); W. Martienssen, Nachr. Akad. Wiss. Göttingen No. 11, 111 (1952); C. J. Delbecq, B. Smaller, and P. H. Yuster, Phys. Rev. 104, 599 (1956).

[13]This topic is made the object of a study by F. Lüty in a manuscript received since the foregoing was written. He focuses attention upon the influence of foreign negative ions on the generation of alpha centers.

LEWIS EFFECT IN RESONANCE YIELD CURVES*

W. L. Walters,† D. G. Costello, J. G. Skofronick, D. W. Palmer, W. E. Kane, and R. G. Herb
Department of Physics, University of Wisconsin, Madison, Wisconsin
(Received September 5, 1961)

Lewis[1] has recently pointed out that a thick-target yield curve taken at a narrow resonance with a charged particle beam of high-energy resolution should have a maximum just above the resonance energy followed by a shallow minimum, before it assumes a constant value. The qualitative explanation for this phenomenon, which the authors have chosen to call "the Lewis effect," is as follows: In passing through target material a charged particle loses energy in discrete steps Q. If some of these steps are larger than the natural width of a narrow resonance, some of the particles incident on a target at an energy well above the resonance energy, E_R, will jump over the resonance. If particles are incident at E_R then all will have for a finite time the correct energy to interact. The yield curve should therefore exhibit a peak near E_R.

Gamma-ray yield curves from the $Al^{27}(p,\gamma)Si^{28}$ resonance reaction at 992 kev were studied with a proton beam having an energy spread at half maximum of about 125 ev. The natural width of this resonance is 80 ± 40 ev.[2] Yield curves were initially taken from aluminum films formed in the target chamber by evaporation of aluminum from a tungsten filament. A peak in the yield curves appeared but could not be reproduced. This was interpreted as being due to the accumulation of surface deposits on the target. A new method of target preparation was developed[3] in which aluminum is slowly and continuously deposited on the target backing while taking data.

Figure 1 shows several yield curves exhibiting the Lewis effect. Curve A is a yield curve calculated as outlined below. The data labelled B and C were taken during continuous evaporation of aluminum. Curves D and E were initial runs from two different targets prepared by filament evaporation; subsequent runs in both cases failed to reveal the Lewis peak.

The yield per proton at a mean beam energy E_b from an infinitely thick homogeneous target is given by

$$Y(E_b) = n_A \int_{E_i=0}^{\infty} \int_{E=0}^{\infty} g(E_b, E_i) \times \sigma(E_R, E)\eta(E, E_i) dE dE_i, \quad (1)$$

where n_A is the number of aluminum atoms per unit volume, $g(E_b, E_i)dE_i$ is the probability that a proton in the beam of mean energy E_b has an incident energy between E_i and $E_i + dE_i$, $\sigma(E_R, E)$ is the cross section for the resonance, and $\eta(E, E_i)dE$ represents the probability that a proton incident at an energy E_i has an energy between E and $E + dE$ somewhere inside the target.

The probability $p(Q, E)dQ$ that a proton at an energy E will suffer a collision in which it loses

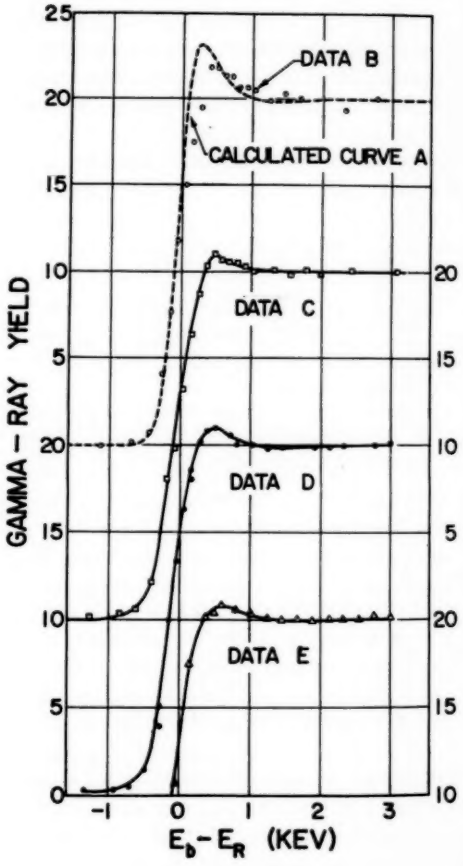

FIG. 1. Thick-target yield curves showing the Lewis effect from the $Al^{27}(p,\gamma)Si^{28}$ resonance at 992 kev. Mean beam energy, E_b, is plotted relative to the resonance energy, E_R. The position of E_R is determined by the calculated yield curve. Plateau yields are normalized for easy comparison of peak amplitudes.

energy between Q and $Q+dQ$ is given by[4]

$$p(Q,E)dQ=(K/EQ^2)dQ, \qquad (2)$$

where K is a constant. Using for this resonance $Q_{min}=12.3$ ev and $Q_{max}=2160$ ev, the function $\eta(E,E_i)$ was numerically calculated on a computer using a Monte Carlo method.

The function $\eta(E,E_i)$ gives the yield per proton at energy E_i from a resonance of infinitesimal width with a monoenergetic beam incident on the target. To account for nonzero resonance width and finite-beam energy resolution, the products of $\eta(E,E_i)$ values and thin-target yield curve values were graphically integrated to give curve A in Fig. 1. The thin-target curve chosen for the calculation was from a target of 60-ev thickness.

Curve A exhibits the peak and shallow minimum predicted by Lewis. The amplitudes of the peaks on experimental yield curves vary by a factor of two. This strongly suggests that surface contamination of the target plays an important role even on targets being continuously evaporated. Some of the discrepancy between the calculated curve of Fig. 1 and the data points B, which exhibit the highest experimentally observed peak, may be attributed to contaminants. On the other hand, the peak in the calculated curve may also be too high because of approximations in stopping-power theory.

The point of half plateau yield on the calculated yield curve, which is commonly assumed to be E_R, does not fall at E_R. For the parameters used here, the half-value point is about 100 ev below E_R.

Experimental work is being extended to other resonance reactions and an attempt will soon be made to utilize higher beam energy resolution. Calculations have shown that the Lewis peak increases in amplitude as resolution improves and as the values of Q_{max} and Q_{min} increase.

---

*This work was supported by the U. S. Atomic Energy Commission and by the Graduate School from funds supplied by the Wisconsin Alumni Research Foundation.

†Present address: Department of Physics, University of Wisconsin–Milwaukee, Milwaukee, Wisconsin.

[1]H. W. Lewis (private communications, 1960-61); Phys. Rev. (to be published).

[2]Jerry B. Marion, Revs. Modern Phys. 33, 139 (1961).

[3]W. L. Walters, Ph.D. thesis, University of Wisconsin, 1961 (unpublished).

[4]Robley D. Evans, The Atomic Nucleus (McGraw-Hill Book Company, New York, 1955), Chap. 18.

ASYMMETRY PARAMETERS IN THE DECAYS $\Sigma^+\to p+\pi^0$ AND $\Lambda\to p+\pi^-$*

E. F. Beall, Bruce Cork,† D. Keefe, P. G. Murphy,‡ and W. A. Wenzel
Lawrence Radiation Laboratory, University of California, Berkeley, California
(Received September 1, 1961)

In recent years, several authors have proposed theories that predict, either on the basis of various forms of global symmetry and the $|\Delta\vec{T}|=\frac{1}{2}$ rule,[1-6] or on the basis of extended chirality invariance,[7] that the asymmetry parameters in the decays $\Sigma^+\to p+\pi^0(\alpha_0)$ and $\Lambda\to p+\pi^-(\alpha_\Lambda)$ should obey the relations $\alpha_0\approx-\alpha_\Lambda$. Here we have

$$\alpha=2\mathrm{Re}(S^*P)/(|S|^2+|P|^2),$$

where S and P are the amplitudes for the two possible angular-momentum channels in each decay. Other theories predict the same sign for α_0 and α_Λ.[8,9] Asymmetry measurements have shown $|\alpha_0|$ and $|\alpha_\Lambda|$ to be large.[10-12] Two published measurements of the sign of α_Λ are in disagreement.[13,14] The experiment reported in this Letter was designed to establish the signs and magnitudes of both α_0 and α_Λ by measuring the polarization of the decay proton from $\Sigma^+\to p+\pi^0$ and $\Lambda\to p+\pi^-$ with a carbon-plate spark chamber.

Figure 1 shows the apparatus used in the experiment. Positive pions of 1.19-Bev/c momentum from the Bevatron were incident upon a liquid-hydrogen target, producing the reactions $\pi^++p\to\Sigma^++K^+$, $\Sigma^+\to p+\pi^0$. During approximately one-third of the run, the hydrogen target was replaced by a block of lithium deuteride. In this case, π^+ mesons of 1.02-Bev/c momentum produced the reactions $\pi^++n\to\Lambda+K^+$, $\Lambda\to p+\pi^-$. The production of a Σ^+ or Λ hyperon was indicated as in earlier experiments[10] by the identification of a K^+ with a counter telescope, including detection of the decay of the K^+ in the large water Čerenkov counter C_K. The hollow-plate spark chamber in the K^+ telescope and the carbon-plate "proton" spark chamber were triggered by a coincidence between the K^+ telescope signal, the signal from the "proton" counter telescope that detected particles with $v/c<0.75$ entering the carbon-plate chamber, and the pulse from a gas Čerenkov

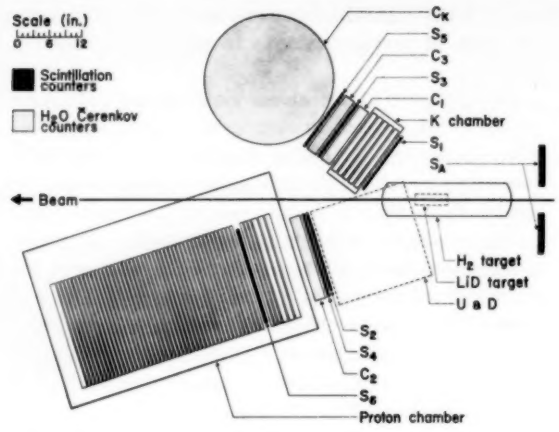

FIG. 1. Plan view of the apparatus used in the experiment. Hyperons were produced either in the H_2 target or in the LiD target. Scintillation counters S_1, S_3, and S_5 detected the K^+ meson; S_2, S_4, and S_6 are scintillation counters that detected the decay proton. The 2-in. water Čerenkov counters C_1, C_2, and C_3 were used to reject particles with $v/c > 0.75$. The water Čerenkov counter C_K stopped the K^+ and detected its decay particle; scintillation counter S_A rejected events not originating in the target; scintillation counters U and D detected pions from Λ decay. The K spark chamber consists of five 1-in. hollow plates with 0.003-in. aluminum surfaces. The proton spark chamber consists of four 1-in. hollow plates and 49 0.5-in. graphite plates sprayed with silver paint. Both chambers were filled with argon.

counter which was located in the incident beam to detect the π^+ meson. Two 90-deg stereo views of each chamber were then photographed. The U and D counters detected those π^- mesons from Λ decay that went approximately up or down with respect to the production plane.

All Σ^+ events with a single proton scattering in the carbon plates of greater than 3-deg projected angle in either view were measured. (Only those events with greater than 5 deg in either view were used in the analysis.) The measured K^+ and proton space angles and proton range allowed us to make a once-overdetermined kinematical fit to the Σ^+ production and decay. The scattering angle and residual range were used to determine the analyzing power of carbon for each event, with the analyzing-power data which have been summarized by Birge and Fowler.[13] Acceptance criteria involving goodness of kinematical fit, maximum and minimum scattering angle, and scattering within a fiducial region of the chamber were imposed. Out of approximately 25 000 pictures, 358 events satisfied all the acceptance criteria and were used as data.

If the polarization of the hyperon is nonzero, the helicity of the decay proton is no longer minus α.[15] However, we have

$$\left[\frac{N(\theta)p_V(\theta) - N(\pi-\theta)p_V(\pi-\theta)}{N(\theta)+N(\pi-\theta)}\right] = -\alpha\cos\theta,$$

where θ is the angle between the proton momentum and the normal to the Σ-K production plane, $p_V(\theta)$ is the polarization of the proton perpendicular to the production plane, and $N(\theta)$ is the number of events. Similarly, we have[16]

$$\left[\frac{N(\theta)p_H(\theta) + N(\pi-\theta)p_H(\pi-\theta)}{N(\theta)+N(\pi-\theta)}\right] = -\alpha\cos\psi,$$

where ψ is the angle between the proton momentum and the direction in the Σ-K production plane which is perpendicular to the hyperon momentum. All of the above quantities refer to the hyperon rest frame. We have used the approximations that the proton and hyperon momenta are parallel in the laboratory system and that the polarization of the proton is the same in the hyperon rest frame as it is in the laboratory system. Therefore, the likelihood functions,

$$L_V(\alpha) = \prod_{i=1}^{358}(1 - \alpha\cos\theta_i A_i \cos\phi_{S_i})$$

and

$$L_H(\alpha) = \prod_{i=1}^{358}(1 - \alpha\cos\psi_i A_i \sin\phi_{S_i}),$$

were computed. Here, A is the carbon analyzing power and ϕ_S is the angle between the plane of scattering and Σ-K production plane. The common logarithms of $L_V(\alpha)$, $L_H(\alpha)$, and $L(\alpha) = L_V(\alpha)L_H(\alpha)$ are plotted in Fig. 2. It should be noted that $L_V(\alpha)$ and $L_H(\alpha)$ independently imply that α_0 is positive. The combined data give $\alpha_0 = +0.75 \pm 0.17$. Corrections for systematic effects have not been included. This value for α_0 agrees well with the lower limit for $|\alpha_0|$ obtained from a measurement of $\alpha_0\bar{p}_\Sigma$ by Cork et al.[10]

Because of the Fermi momentum of the target neutron, we could not use precise kinematical fitting on the Λ events. Therefore, the U and D counters were used to determine whether the π^- meson went up or down with respect to the K^+-π^+

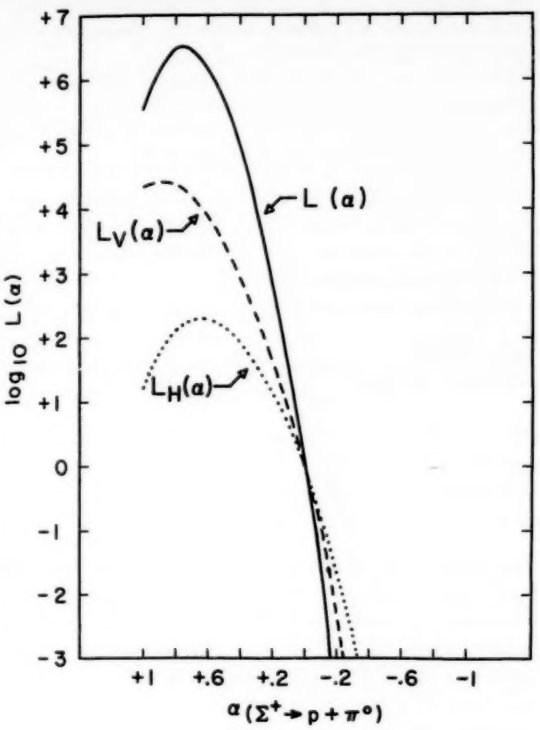

FIG. 2. Common logarithms of the likelihood functions $L_V(\alpha)=\prod_i(1-\alpha A_i\cos\theta_i\cos\phi_{S_i})$, $L_H(\alpha)=\prod_i(1-\alpha A_i\times\cos\psi_i\sin\phi_{S_i})$, and $L(\alpha)=L_V(\alpha)L_H(\alpha)$ for $\Sigma^+\to p+\pi^0$.

plane, and a measurement of the polarization of the proton perpendicular to this plane correlated with the presence of a U or D count allowed a determination of the sign of α from the relation

$$\left[\frac{N_D\langle p_V\rangle_D - N_U\langle p_V\rangle_U}{N_D+N_U}\right]=-\alpha\langle\cos\theta\rangle,$$

with averages taken over all proton directions. From measurements of $\alpha_\Lambda\bar{P}_\Lambda$ by Crawford et al.,[11] it is known that $|\alpha_\Lambda|>0.75\pm0.17$. If it is assumed that $|\alpha_\Lambda|>0.6$, a maximum-likelihood analysis of our data indicates that α_Λ is negative with a confidence of at least 25:1. This result disagrees with the early experiment of Boldt et al.,[14] but agrees with the recent experiments by Birge and Fowler[13] and Leitner et al.[17] Thus, the evidence that α_Λ is large and negative is now quite strong.

The above results imply: (a) The predictions by Nakamura and Konuma[7] that $\alpha_0<0$ and that $\alpha_\Lambda>0$ are in disagreement with experiment. (b) The phenomenological theory by Bludman,[8] which predicts $\alpha_\Lambda\approx+\alpha_0$, is in disagreement with experiment. (c) The S-wave bound-pion model of Barshay and Schwartz[9] (which has been quoted as evidence for odd Σ-Λ relative parity[18]) is also in disagreement with experiment. (d) The evidence that $\alpha_{(\Xi^-\to\Lambda+\pi^-)}$ is positive[19] is strengthened. (e) A fundamental prediction of the global (or doublet) symmetry theories,[1-6] viz., $\alpha_\Lambda\approx-\alpha_0$, is now confirmed.[20]

We are grateful to the many persons who assisted in the building of the equipment, the setting up and operation of the experiment, and the analysis of the data.

---

*Work done under the auspices of the U. S. Atomic Energy Commission.

†Now on leave of absence at the European Organization for Nuclear Research (CERN), Geneva, Switzerland.

‡Work done while on leave from the Rutherford High Energy Laboratory, Harwell, Didcot, England.

[1]R. F. Sawyer, Phys. Rev. 112, 2135 (1958).

[2]B. d'Espagnat and J. Prentki, Phys. Rev. 114, 1366 (1959).

[3]S. B. Treiman, Nuovo cimento 15, 916 (1960).

[4]G. Feldman, P. T. Matthews, and A. Salam, Phys. Rev. 121, 302 (1961).

[5]L. Wolfenstein, Phys. Rev. 121, 1245 (1961).

[6]A. Pais, Phys. Rev. 122, 317 (1961).

[7]S. Nakamura and M. Konuma, Phys. Rev. 122, 1620 (1961).

[8]S. A. Bludman, Phys. Rev. 115, 468 (1959).

[9]S. Barshay and M. Schwartz, Phys. Rev. Letters 4, 618 (1960).

[10]R. L. Cool, B. Cork, J. W. Cronin, and W. A. Wenzel, Phys. Rev. 114, 912 (1959); B. Cork, L. T. Kerth, W. A. Wenzel, J. W. Cronin, and R. L. Cool, Phys. Rev. 120, 1000 (1960).

[11]F. S. Crawford, Jr., M. Cresti, M. L. Good, F. T. Solmitz, M. L. Stevenson, and H. K. Ticho, Phys. Rev. Letters 2, 174 (1959).

[12]F. Eisler, R. J. Plano, A. G. Prodell, N. P. Samios, M. Schwartz, J. Steinberger, P. Bassi, V. Borelli, G. Puppi, G. Tanaka, P. Woloschek, V. Zoboli, M. Conversi, P. Franzini, I. Mannelli, R. Santangelo, and V. Silvestrini, Phys. Rev. 108, 1353 (1957).

[13]R. W. Birge and W. B. Fowler, Phys. Rev. Letters 5, 254 (1960).

[14]E. Boldt, H. S. Bridge, D. O. Caldwell, and Y. Pal, Phys. Rev. Letters 1, 256 (1958).

[15]The general polarization formula has been given, for example, by T. D. Lee and C. N. Yang, Phys. Rev. 108, 1654 (1957).

[16]This relation is rigorous only for $\beta\bar{P}_\Sigma=0$, where $\beta=2\,\mathrm{Im}(S^*P)/|S|^2+|P|^2$. However, β is expected to be small if time-reversal invariance holds.

[17]J. Leitner, L. Gray, E. Harth, S. Lichtman, J.

Westgard, M. Block, B. Brucker, A. Engler, R. Gessaroli, A. Kovacs, T. Kikuchi, C. Meltzer, H. O. Cohn, W. Bugg, A. Pevsner, P. Schlein, M. Meer, N. T. Grinellini, L. Lendinara, L. Monari, and G. Puppi, Phys. Rev. Letters 7, 264 (1961).

[18]Y. Nambu and J. J. Sakurai, Phys. Rev. Letters 6, 377 (1961).

[19]W. B. Fowler, R. W. Birge, P. Eberhard, R. Ely, M. L. Good, W. M. Powell, and H. K. Ticho, Phys. Rev. Letters 6, 134 (1961).

[20]However, the prediction by d'Espagnat and Prentki (reference 2) and Treiman (reference 3) that $\alpha_{(\Xi^- \to \Lambda + \pi^-)}$ and $\alpha_{(\Lambda \to p + \pi^-)}$ have the same sign seems excluded by the results of Fowler et al. (reference 19).

PERIPHERAL COLLISIONS AND THE $(\frac{3}{2}, \frac{3}{2})$ RESONANCE IN THE REACTION $p + p \to n + p + \pi^+$ AT 970 Mev

V. E. Barnes and D. V. Bugg
Cavendish Laboratory, Cambridge, England

and

W. P. Dodd, J. B. Kinson, and L. Riddiford
Department of Physics, University of Birmingham, Birmingham, England

(Received September 13, 1961)

As a continuation of earlier work with a diffusion cloud chamber[1] at the Birmingham University 1-Bev proton synchrotron, proton-proton scattering has been studied with improved accuracy and statistics using a 9-inch liquid hydrogen bubble chamber.[2] Protons were scattered out of the synchrotron at 4° from a carbon target, and the collimated beam was estimated to have an energy spread of ±10 Mev at the bubble chamber. 3007 events within a 1° beam spread and a restricted fiducial region of the chamber have been analyzed so far, yielding the cross sections shown in Table I.

Table I. Cross sections for p-p scattering at 970 Mev.[a]

Reaction	No. of events	Cross section (mb)
(1) $p+p \to p+p$	1554	24.4 ±1.0
(2) $\to d+\pi^+$	35	0.55 ±0.1
(3) $\to p+n+\pi^+$	1170	18.4 ±0.8
(4) $\to p+p+\pi^0$	239	3.8 ±0.35
(5) $\to p+p+\pi^+ +\pi^-$	1	···
(6) $\to p+n+\pi^+ +\pi^0$	1	···
(7) $\to d+\pi^+ +\pi^0$	1	···
Either (3) or (4)	6	···

[a]These cross sections are normalized to a total cross section of 47.3 ±1.0 mb interpolated from the many counter experiments. The elastic scattering cross section includes a correction for scanning losses at very small angles. This table does not include data from the diffusion cloud-chamber experiment, where the number of uncertain events was greater.

In separating reactions (3) and (4), the accuracy of measurement was such that it was frequently necessary to assume only one pion to be created in the interaction and to identify proton or π^+ on the basis of bubble density. However, since only one case of reaction (6) was definitely established, and only one example of double-charged pion production (5) was observed, it is unlikely that the events classed as reactions (3) and (4) contain many cases of double pion production. In only six cases was it impossible to distinguish between (3) and (4). A useful check on the identifications is that the center-of-mass angular distributions were symmetrical backwards and forwards within statistical errors.

Chew and Low[3] have suggested that inelastic reactions in which one pion is created should be strongly influenced at low momentum transfer by poles in the S matrix lying just outside the physical region. The physical interpretation is that there is a large cross section for peripheral collisions of one nucleon with a virtual pion in the field of the other, with a small momentum transfer, Δ, to the latter. In the present experiment there are two poles, since the initial state consists of two protons, and the resulting cross section must be symmetrical between them.

Bonsignori and Selleri[4] have pointed out that, in p-p scattering, peripheral interactions will be most important in reaction (3) where the neutron acts as "spectator" and the proton and π^+ interact in a $T = \frac{3}{2}$ state. They find good agreement with the diffusion cloud chamber results for low momentum transfer. Using this approach, Selleri[5]

has deduced the formula

$$\frac{\partial^2\sigma}{\partial T\partial\omega}=\frac{4f^2m}{\pi p_i^{\,2}\mu^2}\omega R(\omega)\sigma(\omega)[a(T)+b(T,\omega)+c(T,\omega)], \tag{1}$$

where f^2 is the renormalized pion-nucleon coupling constant 0.08, m and μ are the nucleon and pion masses, and p_i is the laboratory momentum of the incident proton. T is the laboratory kinetic energy of the "spectator" nucleon, and ω is the total energy of the pion and the other nucleon in their own rest frame. $\sigma(\omega)$ is the π-nucleon cross section at a center-of-mass energy ω, and the functions R, a, and b are defined by

$$R(\omega)=\tfrac{1}{2}[\omega^4-2\omega^2(m^2+\mu^2)+(m^2-\mu^2)^2]^{1/2}, \tag{2}$$

$$a(T)=\Delta_2^{\,2}/(\Delta_2^{\,2}+\mu^2)^2, \tag{3}$$

$$b(T,\omega)=\Delta_1^{\,2}/(\Delta_1^{\,2}+\mu^2)^2, \tag{4}$$

with

$$\Delta_2^{\,2}=2mT, \tag{5}$$

and

$$\Delta_1^{\,2}=m^2+2m(T_i-T)-\omega^2, \tag{6}$$

where T_i is the laboratory energy of the incident proton. The poles are defined by zeros of the denominators of (3) and (4), and are shown as dashed lines in Fig. 1(a). $c(T,\omega)$ is an interference term between the two poles and is defined in reference 6.

The validity of this theory is clearly demonstrated by Fig. 1(a), where the Q values[6] of $(p\pi^+)$ pairs are plotted against the laboratory energy of the neutron for 1164 events of the type $p+p\rightarrow p+n+\pi^+$. It may be shown that the phase-space factor ρ for this reaction is given by

$$\rho\propto[R(\omega)/\omega]dQdT, \tag{7}$$

being a function of Q only. In Fig. 1(a) the scale has been distorted to allow for this in such a way that points should be uniformly distributed on a statistical basis. The clustering of points close to the phase-space boundaries clearly demonstrates the effects of the poles and the influence of the well-known $(\frac{3}{2},\frac{3}{2})$ resonance at 140 Mev, and it accords reasonably well with the contours of constant cross section calculated from (1) and shown in the figure.

Figure 1(b) compares the experimental values of $d\sigma/dT$ with the predictions of the statistical model and with Selleri's formula. The latter is

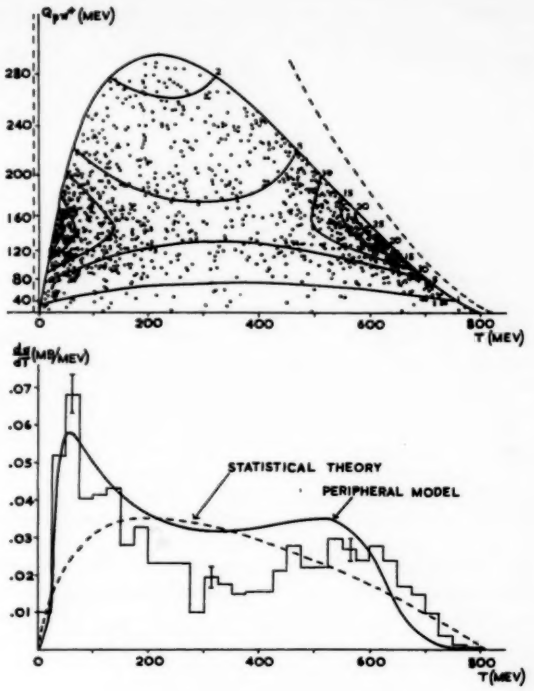

FIG. 1. (a) A scatter diagram of Q values of the $(p\pi^+)$ isobar against neutron laboratory kinetic energy for the reaction $p+p\rightarrow p+n+\pi^+$. The locations of the poles are shown by the dotted lines. Contours of the cross section predicted by Selleri's formula are shown in arbitrary units from 1 to 25. (b) The neutron laboratory energy spectrum compared with Selleri's formula and with phase space normalized to the total number of events.

in good quantitative agreement for momentum transfers less than 600 Mev/c (T less than 180 Mev) and in qualitative agreement for greater momentum transfers. A similar agreement was obtained by Selleri[5] with the diffusion cloud-chamber data.

Using Eq. (1), an attempt has been made to infer the π^+-p cross section using only events with momentum transfer to the neutron less than 430 Mev/c (100 Mev). Events close to both poles have been used by calculating the momentum transfer to each nucleon, and taking the one with the lower value as the "spectator"; this amounts to folding Fig. 1(a) about T values midway between the poles. Since the theory assumes contributions only from the one-pion exchange pole, the agreement shown in Fig. 2 with the known π^+-p cross section (full line) is quite good, and provides some justifica-

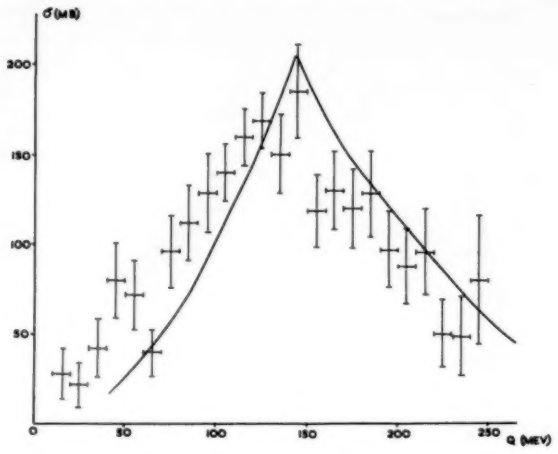

FIG. 2. The cross section for π^+-p scattering inferred from Selleri's formula using only those events in which the momentum transfer to the neutron is less than 430 Mev/c. The full line shows the cross section determined from direct π^+-p scattering experiments.

tion for similar studies of the π-π cross section from inelastic π-p scattering.[7] However, it is found that including events with momentum transfers from 430 Mev/c to 530 Mev/c reduces the agreement of Fig. 2, so that other considerations are necessary in this region. A guide to the magnitude of interference effects is that in the region of momentum transfer up to 430 Mev/c, interference of the amplitude due to the second pole through the term $c(T, \omega)$ in (1) amounts to 5 to 10%, according to the Q value; it has been allowed for in plotting Fig. 2. The original proposal of Chew and Low[3] was to infer the π-p cross section for a number of strips of Δ^2 and to extrapolate to the pole, when interference due to other poles disappears. This has been done by Smith et al.,[8] but there are insufficient events in either their or our experiment to carry out this procedure except in wide intervals of Q.

The comparison of the present results with theory shows clearly that most of the interactions arise from peripheral collisions, thus accounting for the success of the isobar model of Lindenbaum and Sternheimer[1,9] in p-p experiments. For those events with momentum transfers greater than 600 Mev/c, the Q-value distribution is, however, in good agreement with the statistical model. For π-p scattering, where peripheral collisions and isobar formation have different roles, the situation is less clear.[4,10]

We acknowledge the assistance during this work of our colleagues G. A. Doran, S. J. Goldsack, M. Jobes, and B. Tallini at Birmingham, and A. J. Oxley, J. Rushbrooke, and J. Zoll at Cambridge. A full account will be published elsewhere. We are grateful to Dr. L. Castillejo of the Mathematical Physics Department, University of Birmingham, for valuable discussions. D. V. B. and V. E. B. would like to thank Professor O. R. Frisch for helpful criticism.

---

[1]A. P. Batson, B. B. Culwick, J. G. Hill, and L. Riddiford, Proc. Roy. Soc. (London) A251, 218 (1959).

[2]D. C. Colley, J. B. Kinson, and L. Riddiford, Nuclear Instr. 4, 26 (1959).

[3]G. F. Chew and F. E. Low, Phys. Rev. 113, 1640 (1959).

[4]F. Bonsignori and F. Selleri, Nuovo cimento 15, 465 (1960).

[5]F. Selleri, Phys. Rev. Letters 6, 64 (1961). His expression for the cross section is too small by a factor of 2 (recent preprint by Selleri).

[6]$Q = \omega - m - \mu$.

[7]E. Pickup, F. Ayer, and E. O. Salant, Phys. Rev. Letters 5, 161 (1960); J. G. Rushbrooke and D. Radojičić, Phys. Rev. Letters 5, 567 (1960); A. R. Erwin, R. March, W. D. Walker, and E. West, Phys. Rev. Letters 6, 628 (1961).

[8]G. A. Smith, H. Courant, E. Fowler, H. Kraybill, J. Sandweiss, and H. Taft, Phys. Rev. Letters 5, 571 (1960).

[9]S. J. Lindenbaum and R. M. Sternheimer, Phys. Rev. 105, 1874 (1957).

[10]V. Alles-Borelli, S. Bergia, E. Perez Ferreira, and P. Waloschek, Nuovo cimento 14, 211 (1959).

REMARK ON THE ALGEBRA OF INTERACTIONS

A. Pais*
CERN, Geneva, Switzerland
(Received September 8, 1961)

It is the purpose of this note to point out some remarkable similarities between the structure of interactions and the algebra of octonions.

To characterize briefly this strange algebra, we recall some familiar properties of quaternions.

$$X = X_0 e_0 + X_\alpha e_\alpha \tag{1}$$

(summation over $\alpha = 1, 2, 3$) is a quaternion if

$$e_0^2 = 1, \qquad e_0 e_\alpha = e_\alpha e_0,$$

$$e_\alpha e_\beta + e_\beta e_\alpha = -2\delta_{\alpha\beta}, \qquad e_\alpha e_\beta = \epsilon_{\alpha\beta\gamma} e_\gamma. \tag{2}$$

$\epsilon_{\alpha\beta\gamma}$ is totally antisymmetric; $\epsilon_{123} = 1$. If the "components" X_0, X_α are real, define

$$(X, Y) = \tfrac{1}{2}(\bar{X}Y + \bar{Y}X), \quad \bar{X} = X_0 e_0 - e_\alpha X_\alpha, \tag{3}$$

$$N(X) = (X, X). \tag{4}$$

In this real case the norm of the product XS of two quaternions satisfies

$$N(SX) = N(XS) = N(X)N(S), \tag{5}$$

from which by associativity

$$N(S^{-1}XS) = N(X). \tag{6}$$

A null quaternion is defined by

$$X = 0: \; X_0 = X_\alpha = 0. \tag{7}$$

From Eqs. (2) and (3), $(e_\alpha, e_\beta) = \delta_{\alpha\beta}$ so that the three e_α are like orthogonal unit vectors.

Quaternions share with real and complex numbers the property (5). There exists only one other number system[1] (with two variants) for which Eq. (5) is true, namely, the octonions. The first variant satisfies in fact all Eqs. (1)-(7)—with two changes of meaning, however: (a) $\alpha, \beta, \cdots = 1, \cdots, 7$; (b) $\epsilon_{\alpha\beta\gamma}$ is totally antisymmetric and equals +1 for

$$(\alpha\beta\gamma) = (123), (145), (167), (246), (275), (365), (374). \tag{8}$$

Thus one generates octonions from our starting quaternion by introducing a further unit vector e_4, $(e_\alpha, e_4) = 0$, $\alpha = 1, 2, 3$. Then by vector product formation $2e_5 = e_1 \times e_4$, $2e_6 = e_2 \times e_4$, $-2e_7 = e_3 \times e_4$. Equations (2) and (8) show that octonion multiplication is nonassociative and hence does not yield a group.[2] However, any two octonions generate a group; hence Eq. (6) is true as well.

The continuous automorphisms of the e_α form the group G_2. In addition we note the following two discrete operations.

$$P_1: \; e_0 \to -e_0, \tag{9}$$

$$P_2: \; e_\alpha \to ie_\alpha; \quad \alpha = 4, 5, 6, 7; \; i = (-1)^{1/2}. \tag{10}$$

P_1 does not, P_2 does change the multiplication table (8). P_2 adjoins[3] to an X a "split" $X^{(s)}$, $X^{(s)} = X_{re} + iX_{im}$, where X_{re}, X_{im} are orthogonal. Define $N'(X^{(s)}) = N(X_{re}) - N(X_{im})$; then

$$N'(X^{(s)}Y^{(s)}) = N'(X^{(s)})N'(Y^{(s)}),$$

an alternative version of Eq. (5) (second variant).

q-octonions have q-number fields as components. Here too one can define an inner product by taking the Hermitian average on the right side of Eq. (3). Let X be a q-octonion, S a real c-octonion. One shows that Eqs. (5) and (6) are again true. Thus if $N(S) = 1$, then $N(XS) = N(SX) = N(S^{-1}XS) = N(X)$, i.e., one can define octonion gauge transformations of q-octonions.

Let $B = B_0 - ie_\alpha B_\alpha$, $M = M_0 - ie_\alpha M_\alpha$, where the components of $B(M)$ are spin $\frac{1}{2}(0)$ fields. The equation[4]

$$(\gamma\partial + m)B + iG\gamma_5 BM = 0 \tag{11}$$

expresses, by Eqs. (2), (7), and (8), the strong interactions with a high symmetry provided $B_0 = \Lambda$, $2^{1/2}B_1 = \Sigma^+ + \Sigma^-$, $i2^{1/2}B_2 = \Sigma^- - \Sigma^+$, $B^3 = \Sigma^0$, $i2^{1/2}B_4 = n + \Xi^0$, $-2^{1/2}B_5 = p + \Xi^-$, $i2^{1/2}B_6 = p - \Xi^-$, $-2^{1/2}B_7 = n - \Xi^0$. Put $B = B(\Lambda, \Sigma, N, \Xi)$. Then[5]

$$M = B(\sigma, \pi, K, K^G). \tag{12}$$

The M components are eigenstates of charge conjugation. The "full symmetry" is: global symmetry of the type[6] G^- and moreover K-coupling strengths = minus π-nucleon coupling.

Thus the octonion calculus which involves sets of eight "equivalent particles" automatically pro-

duces all needed selection rules plus those unwanted extra ones implied by too strong a symmetry. We now observe that we can adjoin to B two other octonions, namely $B^{(1)}=P_1B$ and $B^{(2)}=P_2RB$, where $R=(e_7\to e_4,\ e_4\to -e_7,\ e_5\to e_6,\ e_6\to -e_5)$ and is in G_2. Replace in Eq. (11) BM by $[B+c_1B^{(1)}+c_2B^{(2)}]M$ and the following happens: In the right qualitative way, the baryon masses split as $8=1+3+2+2$, the meson masses as $8=1+3+4$. Each of the three couplings separately have equivalent full symmetry, denoted by F, $F^{(1)}$, $F^{(2)}$, respectively. Some partial symmetries are: $F+F^{(2)}$ = doublet approximation, $F+F^{(1)}$ = Behrends-Sirlin scheme.[7] Note that three is the minimal number of clashing full symmetries which breaks the degeneracies.[8] The usual charge operator

$$Q=T_3+Y_3 \tag{13}$$

is the sum of the third components of isotopic spin and hyperspin and has the following curious property. With respect to each of the F's separately, Q itself is isomorphic to a third component of angular momentum. (This is not true for any other nontrivial linear combination of T_3 and Y_3.)

The above example of the lifting of degeneracies is not unique. In particular, the present calculus is not tied to the strange particle parities.[9]

Consider next the transformations

$$B\to S^{-1}BS,\quad M\to S^{-1}MS, \tag{14}$$

with S a real c-octonion, $N(S)=1$. By application of G_2, S can be brought into the canonical form $S=\exp e_4\xi$. For infinitesimal ξ, the transformation (14) is not in G_2. Even so, Eq. (11) with $G=0$ is invariant under Eq. (13) as S, B generate a group. For $G\neq 0$, Eq. (11) becomes $(\gamma\partial+m)B+S[(S^{-1}BS)\times(S^{-1}MS)]S^{-1}=0$. For "infinitesimal" ξ one finds that now $BM\to BM+$"weak" interaction with $\Delta T=\frac{1}{2}$. Thus e_4 acts as the spurion. For the present we do not discuss the parity structure of weak nonleptonic interactions so generated.

If the octonion algebra envelops in some sense the structure of interactions, one may ask how the leptons could enter. Here the electric charge should form one bridge. Especially if two neutrinos ν_1, ν_2 exist, it is interesting to contemplate the possibility that, rather like M, the lepton is a self-charge conjugate octonion L. L can be so constructed that, where $(B,Q\gamma_\lambda B)$ is the electric baryon current, so $(L,Q\gamma_\lambda L)$ is the electric lepton current. In treating neutral leptons considerable arbitrariness exists, however, partly connected with the group $SU(3)$ (subgroup of G_2) of automorphisms which keep one e_α fixed. Lepton conservation induces insufficient restrictions. Some partial results follow.

Using doublet language,[10] write B as $B(N_1,N_2,N_3,N_4)$. Put[11]

$$L(\omega)=2^{-1/2}B(\omega n_4{}^C,\ -\omega n_3{}^C,n_3,n_4), \tag{15}$$

$$n_3=\begin{pmatrix}\nu_1\\ e\end{pmatrix},\quad n_4=\begin{pmatrix}\nu_2\\ \mu\end{pmatrix}.$$

ω is a 2×2 unitarity matrix; $(\omega^\dagger\tau_3\omega)^T=-\tau_3$. As for B, one checks that Q is indeed the L electric charge operator.

Define current octonions[12] $J=\bar{L}\gamma L$, $j=\bar{B}\gamma(1+\alpha\gamma_5)\times B$. The inner product,

$$(J,j)=\sum_{a=0}^{7}J_a{}^Cj_a,$$

describes leptonic transitions, as follows. $a=0,3$: $\Delta S=0$, neutral; $a=1,2$: $\Delta S=0$, charged; $a=4,7$: $|\Delta S|=1$, neutral; $a=5,6$: $|\Delta S|=1$, charged. One finds $J_0=J_4=J_7\equiv 0$ for any ω as defined. Hence there are no neutral $|\Delta S|=1$ transitions. Let $J^{(1)}$ correspond to $\omega=i\tau_1$. One finds $J_5{}^{(1)}=J_6{}^{(1)}=0$. Thus $(J^{(1)}+j,J^{(1)}+j)$ describes the universal $\Delta S=0$ interaction.[13] Let $J^{(2)}$ refer to (a) interchange of ν_1 with $\nu_i{}^C$, ν_2 with $\nu_j{}^C$, $(i\neq j)=1,2$; (b) $\omega=i\tau_1$. One finds $J_1{}^{(2)}=J_2{}^{(2)}=0$, while now $J_5{}^{(2)}$, $J_6{}^{(2)}$ are lepton-conserving $|\Delta S|=1$ charged currents. The two choices for (i,j) are related to the neutrino-flip question.[14] It is perhaps a good aspect that the absence of $|\Delta S|=1$ neutral leptonic follows from a specific algebra. It is perhaps a bad aspect that the synthesis of $\Delta S=0$ leptonic and $|\Delta S|=1$ is so far not unique. (The use of different L's is not unlike the use of different B's for strong interaction asymmetries.)

It should be noted that all results stated here could have been written without using octonions at all. The formal structure here described seemed sufficiently intriguing to communicate, however. Yet the close connection between octonion algebra and some aspects of the interactions may be nothing but a strange coincidence. To be more than that, this algebra should play a dynamical role.[15]

The author is much indebted to CERN for its hospitality and financial support. He also wishes to acknowledge a consultation with I. Ching.

*Permanent address: Institute for Advanced Study, Princeton, New Jersey.

[1]Hurwitz' theorem. For early developments see L. Dickson, Ann. Math. 20, 155 (1918). For both variants the components are real (real octonions).

[2]But rather a so-called quasi-group where the associative law is replaced by a certain weaker law. For the present it suffices to state that for octonions this law is: The associator $X(YZ)-(XY)Z$ is totally antisymmetric in X,Y,Z.

[3]In this case and also for the q-octonions mentioned below, we have no longer a division algebra. This does not matter as we need not take inverses of wave fields.

[4]For the purpose of exposition we consider only trilinear interactions and leave aside the question whether strong interactions are generated by gauge fields.

[5]σ is a $T=S=0$ meson conjectured by many authors. $\sigma \equiv 0$ is not necessarily excluded. $K=(K^+,K^0)$; $K^G=(-\bar{K}^0,K^-)$.

[6]In a terminology employed elsewhere; A. Pais, Phys. Rev. 122, 317 (1961).

[7]R. Behrends and A. Sirlin, Phys. Rev. 121, 324 (1961).

[8]Example: $B^{(3)}=R'B$; $R'=(e_\alpha \rightarrow -e_\alpha)$, $\alpha=4,5,6,7$ and is in G_2. Even with all these couplings there remains a simple π-coupling constant relation: $(NN\pi)=-(\Sigma\Sigma\pi)=(\Xi\Xi\pi)$. Note: P_1 corresponds essentially to $BM \rightarrow MB$.

[9]Example: Write the above B as $B(N,\Lambda,\Sigma,\Xi)$, define $B'=B(N,c_1\gamma_5\Lambda,\Sigma,c_2\gamma_5\Xi)$, and replace in Eq. (11) BM by $B'M$. This spreads the masses due to space parity effects. The curious property of Q is now lost. The example in the text may be said to generate splits due to two "isotopic parities."

[10]In the notation of reference 6. As is done in part of the quoted paper, the doublets are used as a mathematical device without necessarily insisting on any mass degeneracy.

[11]C = charge conjugate. $\nu_i=\frac{1}{2}(1+\gamma_5)\psi_i$. ψ_i is a massless spinor. It is possible but unattractive to put $\nu_1 \equiv \nu_2$. T = transpose.

[12]The four-vector index is suppressed. J will always have the correct V-A combination due to the very definition of ν_i. The j_α, $\alpha=4,5,6,7$, have $\Delta T=\frac{1}{2}$. Also $\Delta T=\frac{3}{2}$ currents can be constructed, namely by using G_2 generators; see reference 7.

[13]Including a neutral $\Delta S=0$ current $J_3^{(1)}$ without $\mu\epsilon$ terms. To such a current there is so far no objection; see S. Bludman, Phys. Rev. 115, 468 (1959). (In the present case the $\bar{\mu}\mu$ and $\bar{e}e$ terms moreover conserve parity.) For a first attempt to tie lepton phenomena to a group, see S. Bludman, Nuovo cimento 9, 433 (1958).

[14]G. Feinberg, F. Gürsey, and A. Pais, Phys. Rev. Letters 7, 208 (1961). Another ambiguity exists due to the fact that j need not necessarily be the same for $\Delta S=0$ as for $\Delta S=1$.

[15]Note the possibility of linearized octonion wave equations. Let X be an octonion field, $O=e_\mu p_\mu+ie_\rho m_\rho+m_0$, $\mu=1$-4, $\rho=5$-7, m_ρ mass parameters. Put $OX=0$. Then $\bar{O}(OX)=(\bar{O}O)X=0$. Hence we get a standard wave equation for mass $(m_\rho^2+m_0^2)^{1/2}$, for each component of X.